Complementarity Models for Traffic Equilibrium with Ridesharing

Huayu Xu[*], Jong-Shi Pang[†], Fernando Ordóñez[‡], and Maged Dessouky[§]

Original April 2015; revised July 2015; final August 2015

Abstract

It is estimated that 76% of commuters are driving to work alone while each of them experiences a 38-hour delay annually due to traffic congestion. Ridesharing is an efficient way to utilize the unused capacity and help with congestion reduction, and it has recently become more and more popular due to new communication technologies. Understanding the complex relations between ridesharing and traffic congestion is a critical step in the evaluation of a ridesharing enterprise or of the effectiveness of regulatory policies or incentives to promote ridesharing. The objective of this paper is to introduce a mathematical framework for the study of the ridesharing impacts on traffic congestion and to pave the way for the analysis of how people can be motivated to participate in ridesharing, and conversely, how congestion influences ridesharing activities. We accomplish this objective by developing a new traffic equilibrium model with ridesharing, and formulating the model as a mixed complementarity problem (MiCP). We provide conditions on the model parameters under which there exists one and only one solution to this model. The computational results show that when the congestion cost decreases or the ridesharing inconvenience cost increases, more travelers would become solo drivers and thus less people would participate in ridesharing. On the other hand, when the ridesharing price increases, more travelers would become ridesharing drivers.

1 Introduction

For many years traffic congestion has been a significant transportation problem, especially in large urban areas, and congestion reduction has been a hot but tough issue in both academic research and city planning. According to The 2012 Annual Urban Mobility Report [33], it is estimated that (a) the average annual delay endured by each commuter was 38 hours (compared to 16 hours in 1982), and (b) the annual cost of congestion is more than $120 billion–nearly $820 for every commuter in the United States. The expansion speed of the population of commuters is always one step ahead of the infrastructure capacity. At the same time, according to the Transportation Statistics Annual Report 2012 by the Bureau of Transportation Statistics [5], 76.4% of commuters

[*]The Daniel J. Epstein Department of Industrial and Systems Engineering, University of Southern California, Los Angeles, California 90089-0193 U.S.A. Email:cxuhuayu@gmail.com.

[†]The Daniel J. Epstein Department of Industrial and Systems Engineering, University of Southern California, Los Angeles, California 90089-0193, U.S.A. The work of this author was based on research supported by the U.S. National science Foundation under grant CMMI-1402052. Email: jongship@usc.edu.

[‡]Industrial Engineering Department, Universidad de Chile, Republica 701, Santiago, Chile. Email: fordon@dii.uchile.cl.

[§]Corresponding author. The Daniel J. Epstein Department of Industrial and Systems Engineering, University of Southern California, Los Angeles, California 90089-0193 U.S.A. The research of this author was supported by the Federal Highway Administration under the Broad Agency Announcement of Exploratory Advanced Research. Email: maged@usc.edu.

drove to work alone in 2011. Therefore there exists an urgent need to tap into such a significant amount of unused capacity in transportation networks.

Ridesharing, or carpooling, appears as one such innovative transportation mode that could help fulfill such a need and also mitigate the congestion increase. Benefits of ridesharing include travel cost savings, reducing travel time, mitigating traffic congestion, conserving fuel, and reducing air pollution [9, 15, 22, 29]. Recently, technological advances including global positioning systems (GPS) and mobile devices have greatly enhanced the communication capabilities of travelers, facilitating the creation of ridesharing in real-time. Taking advantage of this opportunity, a number of companies, such as Uber, Lyft, Avego (Carma), SideCar, etc., have emerged to develop systems where travelers (including both drivers and passengers) can be matched in real time via mobile apps [17]. In a sense these companies are establishing a marketplace for drivers to offer up their empty seats to other travelers. The essential difference of such ridesharing systems from traditional public transit systems is that they do not hire professional drivers and they function as a matching agency that pairs passengers with "citizen" drivers.

In a previous paper [37], we studied a transportation system where ridesharing has the ability of capturing a significant portion of travel demand via a real-time matching agency. In this ridesharing system, we assume that the passengers will pay the drivers for the ridesharing services to share the travel cost. The ridesharing price is an abstraction to represent compensation that drivers take into account in their decision to participate in ridesharing, such as a reduction in travel time or toll costs that will occur by being able to use high-occupancy vehicle (HOV) lanes. We also assume that the system operates as an open marketplace and thus the ridesharing price will be determined by the market, e.g. the drivers and passengers that are participating in ridesharing. In our previous paper, for simplicity we assumed that drivers and passengers who share the same vehicle must be traveling from the same origin to the same destination. In this paper, we focus on relaxing this assumption to develop a more general and representative mode of ridesharing. As is in most realistic ridesharing scenarios, drivers may make a detour, slight or big, to pick up or drop off some passenger(s).

The purpose of this paper is to determine how people will behave where there exists such a ridesharing market, and furthermore determine how ridesharing activities would impact the traffic congestion. The travelers are categorized in three types: (a) *solo drivers* who drive alone, (b) *ridesharing drivers* who share their car, and (c) *passengers* who take a ride. The major decision factors for the travelers to choose their traveling types include the traffic congestion, the ridesharing price and the inconvenience caused by ridesharing activities. For instance, to decide whether to participate in ridesharing, drivers may weigh the inconvenience, such as loss of privacy, against the compensation they may earn for taking on passengers. In turn, passengers would tradeoff the inconvenience, such as security concerns and loss of freedom, against the travel time and cost of a shared ride. These tradeoffs would balance in an equilibrium that determines the traffic congestion, the ridesharing prices, and the number of different types travelers. For example, an increase in ridesharing (more passengers) could lead to a reduction in congestion, which in turn makes it less stressful to be a driver, leading to an increase in drivers and thus an increase in congestion. Understanding how ridesharing would influence traffic congestion is fundamental in the evaluation of a ridesharing enterprise or in assessing the effectiveness of regulatory policies or incentives to promote ridesharing.

Obviously, a ridesharing system, due to the individual roles of the three types of travelers, is distinct from a multi-modal transportation system wherein passengers can select multiple modes of travel on a trip, but the modes selected do not influence the capacity or cost of alternative modes of

travel. In a ridesharing system, a driver can decide to pick up passengers, which influences the availability and costs of shared rides.

However, we do not include a detailed assignment of passengers to vehicles. We are only modeling the behavior of the aggregate quantities of drivers and passengers. In the proposed model there only exist ridesharing passengers on an arc (road segment) if there are ridesharing drivers traversing the corresponding arc. A certain passenger can be taken only if there is enough capacity on the corresponding ridesharing vehicles. If there are none, then the traveler has the options to be a solo driver or ridesharing driver and would select the one that is less expensive.

The paper is organized as follows. Section 2 presents a literature review, including both ridesharing systems and traffic assignment problems. Section 3 models our ridesharing system as a mixed complementarity problem and Section 4 presents the computational results and analysis. We finish the paper with conclusions in Section 5.

2 Literature Review

Ridesharing is a joint-trip of at least two participants that share a vehicle and requires coordination with respect to itineraries [17]. Some ridesharing services occur spontaneously among individual travelers motivated by access to faster HOV (High-Occupancy Vehicle) lanes or reduced tolls. Examples of this type of ridesharing service are casual carpooling [6, 22], and slugging, which formed in the Washington D.C. area free of charge to the participants [26, 34]. These services run on their own momentum; they are not started or run by a public or private entity [27]. Therefore they are limited to specific locations or circumstances and are difficult to replicate elsewhere.

With innovative technologies inhibitors of ridesharing can be overcome and a number of private matching agencies have emerged during the last decade [3, 9, 12, 18, 20]. Such ridesharing services are operated by agencies that provide ride-matching opportunities for participants without regard to any previous historical involvement [12]. By introducing mobile technologies like smart phones as well as global positioning systems (GPS), ridesharing systems can be implemented in real-time. This allows matching agencies to incorporate current locations and travel itineraries in better proposals to travelers, which could lead to increasing the degree of adoption of ridesharing systems.

However, the literature discussing the relationship or the interaction between ridesharing activities and traffic congestion is quite limited. The paper [38] discussed the carpooling behavior and the optimal congestion pricing in a multilane highway with or without HOV lanes where the first-best pricing and the second-best pricing models were formulated and compared. The models, however, were limited to identical commuters (single origin and single destination, SOSD) and the number of passengers in each carpooling vehicle is fixed to one. The paper [32] studied the morning commute problem with three modes: transit, driving alone and carpool. The authors analyzed the interactions among the three modes and how different factors affect their mode shares and network performance. Again, the model is limited to a SOSD network and does not consider the interactions of ridesharing between different origin-destination (OD) pairs.

To study the effects of multiple OD pairs, one classic model is the traffic assignment problem (TAP) [31], which evaluates the distribution of travelers among different routes and OD pairs. The basic assumption underlying this problem is the renowned Wardop's user equilibrium principle [35] which postulates that the travel times (congestion costs) in all the used paths are equal and not more than those that would be experienced by a vehicle on any unused path. Mathematically, this principle is the cornerstone to the complementarity and variational inequality approach of

the user equilibrium (UE) problem pioneered by Aashitiani and Magnanti [1] and Dafermos [11]; see [14, Section 1.4.5] for details of this approach and the Notes and Comments Section 1.9 for a historical account and more references on this problem. Recent references include [2, 4, 28, 30] as well as some recent work on the continuous-time versions of the dynamic UE mentioned before. In [37], an optimization model was introduced for the ridesharing traffic assignment problem under the assumption of no detours for passenger pick up and drop off. When the latter assumption is removed, the optimization framework is no longer applicable and we need to resort to a variational inequality (VI) or its equivalent complementarity formulation. The cited paper also treats the case of elastic demands by introducing a utility for travel; the problem decides not only how people will choose their paths, but also how many people would travel given certain congestion conditions. This kind of model serves to illustrate those cases where people might not travel when the traffic is highly congested. While the VI approach can treat elastic demands in the ridesharing framework, we will focus on the fixed-demand ridesharing model in this paper.

3 Mathematical Model

The ridesharing equilibrium problem with multiple OD pairs is not amenable to solution as an optimization problem because it lacks an obvious objective function. Instead, we formulate the problem as a mixed complementarity problem. This allows us to determine the type (solo driver, ridesharing driver, or passenger) a traveler chooses to be and to understand the relations between ridesharing activities and traffic congestion when such conditions change.

Our roadmap to the analysis of a ridesharing user equilibrium is as follows. We first introduce an expanded network to model the ridesharing paradigm; this is followed by a formal definition of a ridesharing user equilibrium and its natural formulation as a mixed complementarity problem (in terms of *path* flows) whose solution is shown to yield such an equilibrium. Next, it is shown that the *arc* flows induced by such equilibrium path flows must be a solution to a variational inequality (VI). We show that the latter VI has a unique solution under a set of mild conditions on the model constants. The upshot of this uniqueness result is that while the path flows of a ridesharing user equilibrium are not necessarily unique, under some mild conditions, there is a unique set of arc flows induced by any such (path-flow) equilibrium. This uniqueness conclusion extends to the ridesharing case a known result of traffic equilibrium. Some numerical examples are presented to illustrate the overall approach.

Consider a transportation network represented by a graph with nodes and arcs, where nodes could be origins, destinations or intermediate stops, and arcs are direct roads that connect two nodes. Each individual travels from an origin to a destination, which is called an origin-destination (OD) pair. For each OD pair, there exist multiple paths that start from the origin and end at the destination. Travelers are categorized into three groups: solo drivers, ridesharing drivers and passengers. They experience different costs due to different paths and different roles. More specifically, we assume that:

• **There are three traveler roles: solo drivers, ridesharing drivers and passengers.**

• **Drivers may pick up or drop off any passenger(s) at any time anywhere.** That is to say, drivers and passengers who are sharing the same vehicle may or may not travel on the same OD pair. Drivers may even detour for a passenger if needed.

• **All drivers must be driving throughout their trips.** Solo drivers and ridesharing drivers may switch roles (when picking up or dropping off passengers in the middle of their trips), but

neither can become a passenger.

• **All passengers must remain passengers throughout their trips.** They cannot become a driver in the middle of trips once they have decided to travel as a passenger.

• **The total number of travelers of each OD pair is fixed.** However, for each traveler, they may decide to be a solo driver, a ridesharing driver or a passenger.

• **The vehicle capacity is limited and fixed for all ridesharing vehicles.** In other words, the number of passengers in each vehicle cannot exceed a given limit.

We note that since travelers experience different costs due to different paths and different roles, travelers could face different costs even on the same path. Therefore travelers select the path and role that give them the least cost, impacting other travelers' costs, until an equilibrium is reached. Given the above assumptions, our goal is to derive a model that determines how travelers will choose their **roles** and their **paths** given certain conditions. Note that it is difficult to capture or iterate the travel information for each driver. A driver may travel alone in the first half of their trip and then pick up some passenger(s) and share the ride till the end of their trip. That means, the driver's path is a mix of "driving alone" and "taking on passenger(s)". Therefore we need to construct an extended network that may capture the information of such mixed paths. Before introducing such a network and the notation, we present a formal definition of the finite-dimensional variational inequalities (VIs) and complementarity problems (CPs) that provide the key mathematical formulations for this study.

3.1 The VI/CP

We use the notation $x \perp y$ for x and y in $\mathbb{R}^n$ to denote that they are perpendicular vectors, that is $x^T y = 0$. For given vector-valued functions $F : \mathbb{R}^{n+m} \to \mathbb{R}^n$ and $G : \mathbb{R}^{n+m} \to \mathbb{R}^d$, the mixed complementarity problem (MiCP) is that of finding a pair of vectors $(x, y) \in \mathbb{R}^{n+m}$ satisfying $0 \leq x \perp F(x, y) \geq 0$ and $G(x, y) = 0$ with the former meaning the three conditions $x \geq 0$, $F(x, y) \geq 0$, and $x^T F(x, y) = 0$. For a given mapping $\Phi : K \subseteq \mathbb{R}^N \to \mathbb{R}^N$, the variational inequality VI(K, Φ) is the problem of finding a vector $z \in K$ such that $(z' - z)^T \Phi(z) \geq 0$ for all $z' \in K$. Results about these two problems will be used freely in this paper; see [14] for a reference. In particular, it is known that if K is a convex compact set and Φ is continuous then VI(K, Φ) has a solution. If in addition the operator Φ is *strictly monotone* on K, i.e., if

$$(z - z')^T(\Phi(z) - \Phi(z')) > 0, \quad \forall z \neq z' \text{ in } K,$$

then the VI (K, Φ) has a unique solution. In turn, if Φ is continuously differentiable and the Jacobian matrix $J\Phi(x)$ of Φ is positive definite for all $z \in K$, then Φ is strictly monotone on K.

3.2 Construction of the Extended Network

Note that drivers and passengers are unexchangeable, hence we need to split each node (and accordingly, each arc) into two to separate drivers and passengers. Also note that we have two types of drivers: solo and ridesharing drivers, we need to split again each "driver" arc into two. We do not need to split nodes for different types of drivers, since solo drivers and ridesharing drivers are exchangeable. They need to share the nodes in order to switch roles, where the nodes connect both "solo-driver" arcs and "ridesharing-driver" arcs.

For example, in Figure 1 (a), the original graph consists of nodes i, j and k, and arcs (i, j) and (j, k). The extended graph (see Figure 1 (b)) therefore consists of

- "driver" nodes i, j and k;
- "passenger" nodes i', j' and k';
- "solo-driver" arcs (i, j) and (j, k) (solid line);
- "ridesharing-driver" arcs (i, j) and (j, k) (dashed line)
- "(ridesharing-)passenger" arcs (i', j') and (j', k') (dotted line).

More specifically, suppose the original graph is $\mathcal{G}_0 = (\mathcal{N}_0, \mathcal{A}_0)$, where $\mathcal{N}_0$ and $\mathcal{A}_0$ represent the original node set and arc set, respectively. The extended graph $\mathcal{G} = (\mathcal{N}, \mathcal{A})$ is therefore given by:

- Let $\mathcal{N} \triangleq \mathcal{N}_0 \cup \mathcal{N}_0'$ be the extended node set, where $\mathcal{N}_0$ represents the "driver" nodes and its duplicate $\mathcal{N}_0'$ represents the "passenger" nodes;
- Let $\mathcal{A}_1 \triangleq \mathcal{A}_0, \mathcal{A}_2 \triangleq \mathcal{A}_0$ be the "solo-driver" arcs and "ridesharing-driver" arcs, respectively;
- Let $\mathcal{A}_3 \triangleq \mathcal{A}_0' = \bigcup_{(i,j)\in\mathcal{A}_0} \{(i', j')\}$ be the "passenger" arcs.

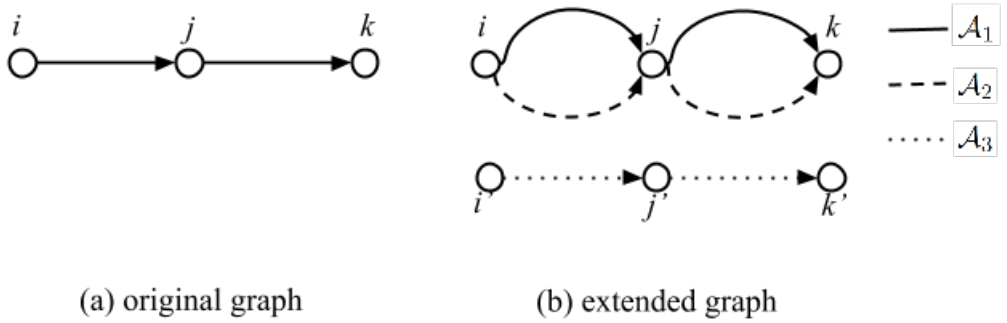

Figure 1: Graph extension

It looks as if we simply duplicated the original graph to two separate graphs. As a matter of fact, these two "separate" graphs are connected by the fixed demands, i.e. the sum of flows running out of the two split origin nodes (or running into the two split destination nodes) should be fixed.

Therefore, travelers may start at either node i if they wish to drive, or node i' if they want to take a ride. If they pick the driver node i to start, they can travel on arc $a_1 \in \mathcal{A}_1$ and/or arc $a_2 \in \mathcal{A}_2$ before they reach the destination node $k \in \mathcal{N}_0$. For example, in Figure 1, a traveler may be driving along the solid arc (i, j) and then the dashed arc (j, k). This means that he/she drives alone from node i to j and then picks up some passenger(s) to share a ride from j to k (and drop off the passenger(s) at k). But drivers cannot travel to passenger arcs (dotted arcs) once they choose to start from a driver node. It is because we assume that drivers cannot leave their vehicles at a node other than their destinations.

Similarly, once travelers start at a passenger node i', they can only travel on arc $a_3 \in \mathcal{A}_3$ before they reach their destination, which is also a passenger node $k' \in \mathcal{N}_0'$. There exists no arc connecting a passenger node in $\mathcal{N}_0'$ to a driver node in $\mathcal{N}_0$. This is because we assume that travelers cannot start driving a vehicle from a node other than their origin.

3.3 Summary of Notations

Below is a list of notations that we use to formulate a fixed-demand, ridesharing TAP model.

Network structure

$\mathcal{G}_0 = (\mathcal{N}_0, \mathcal{A}_0)$	original network with the node set $\mathcal{N}_0$ and the arc set $\mathcal{A}_0$
$\mathcal{G} = (\mathcal{N}, \mathcal{A})$	extended network with the node set $\mathcal{N}$ and the arc set $\mathcal{A}$
$\bar{\mathcal{O}}, \bar{\mathcal{D}} \subseteq \mathcal{N}_0$	original sets of origins and destinations, respectively
$\mathcal{O}, \mathcal{D} \subseteq \mathcal{N}$	extended sets of origins and destinations, respectively, where $\mathcal{O} \triangleq \bar{\mathcal{O}} \cup \bar{\mathcal{O}}'$ and $\mathcal{D} \triangleq \bar{\mathcal{D}} \cup \bar{\mathcal{D}}'$
$\mathcal{K} \subseteq \mathcal{O} \times \mathcal{D}$	set of OD pairs $\mathcal{K} = \{(o_k, d_k), (o'_k, d'_k) \mid o_k \in \bar{\mathcal{O}}, d_k \in \bar{\mathcal{D}}, o'_k \in \bar{\mathcal{O}}', d'_k \in \bar{\mathcal{D}}'\}$, including both driver and passenger OD pairs
$\mathcal{A}_1, \mathcal{A}_2, \mathcal{A}_3$	sets of arcs of solo drivers, ridesharing drivers, and passengers, respectively, $\mathcal{A} = \mathcal{A}_1 \cup \mathcal{A}_2 \cup \mathcal{A}_3$
a_1, a_2, a_3	arcs representing solo drivers, ridesharing drivers and passengers, respectively, $a_j \in \mathcal{A}_j, j = 1, 2, 3$
D_k	total demand of travelers (including all drivers and passengers) for OD pair k, assumed to be a fixed constant
C	ridesharing capacity, $C > 1$; i.e., the maximum number of passengers in each vehicle
IN(i), OUT(i)	sets of arcs entering and leaving node $i \in \mathcal{N}$, respectively
$\mathcal{T}_j(a_0)$	mapping an original arc $a_0 \in \mathcal{A}_0$ to its corresponding arc $a_j \in \mathcal{A}_j$, $j = 1, 2, 3$ i.e. $\mathcal{T}_j : \mathcal{A}_0 \to \mathcal{A}_j$
$\mathcal{T}_0(a)$	mapping an arc $a \in \mathcal{A}$ to the original arc $a_0 \in \mathcal{A}_0$ it is generated from i.e. $\mathcal{T}_0 : \mathcal{A} \to \mathcal{A}_0$
p	a path that consists of one or several consecutive arcs;
$\mathcal{P}_k$	set of paths for OD pair k, i.e. set of all paths that either start at o_k and end at d_k or start at o'_k and end at d'_k
$\mathcal{P} \triangleq \bigcup_{k \in \mathcal{K}} \mathcal{P}_k$	set of all paths in the network (for all OD pairs).

Since $\mathcal{A}_1, \mathcal{A}_2 \subset \mathcal{N}_0 \times \mathcal{N}_0$ and $\mathcal{A}_3 \subset \mathcal{N}'_0 \times \mathcal{N}'_0$, a path p will either only visit nodes in $\mathcal{N}_0$ using arcs from $\mathcal{A}_1$ or $\mathcal{A}_2$ or only visit nodes in $\mathcal{N}'_0$ using arcs in $\mathcal{A}_3$. Thus a path p can contain only arcs of type $\mathcal{A}_3$ or only arcs in $\mathcal{A}_1 \cup \mathcal{A}_2$.

Model Variables

x_a^k	amount of flow for OD pair $k \in \mathcal{K}$ on arc $a \in \mathcal{A}$
$y_a = \sum_{k \in \mathcal{K}} x_a^k$	total amount of flow on arc $a \in \mathcal{A}$
$\eta_{a_0}^{\pm}$	compensation of ridesharing capacity on link $a_0 \in \mathcal{A}_0$
u_k	minimum generalized travel costs between OD pair $k \in \mathcal{K}$
h_p	amount of flow on path p, i.e. the amount of flow that travels from o_k (or o'_k) to d_k (or d'_k), for any $k \in \mathcal{K}$ and $p \in \mathcal{P}_k$
$\boldsymbol{x}^k \in \mathbb{R}^{\lvert\mathcal{A}\rvert}$	vector with components x_a^k for $a \in \mathcal{A}$
$\boldsymbol{x} \in \mathbb{R}^{\lvert\mathcal{K}\rvert\lvert\mathcal{A}\rvert}$	vector with components x_a^k for $a \in \mathcal{A}$ and $k \in \mathcal{K}$
$\boldsymbol{y} \in \mathbb{R}^{\lvert\mathcal{A}\rvert}$	vector with components y_a for $a \in \mathcal{A}$
$\boldsymbol{\eta}^{\pm}$	vector with components $\eta_{a_0}^{\pm}$ for $a_0 \in \mathcal{A}_0$
$\boldsymbol{u} \in \mathbb{R}^{\lvert\mathcal{K}\rvert}$	vector with components u_k for $k \in \mathcal{K}$
$\boldsymbol{h} \in \mathbb{R}^{\lvert\mathcal{P}\rvert}$	vector with components h_p for $p \in \mathcal{P}$.

3.4 Cost Functions

The cost functions of each arc a in this model are defined as below.

• *Congestion cost for drivers* (experienced by every solo or ridesharing driver): The classic BPR (Bureau of Public Roads) arc cost function is adopted here. The congestion cost is calculated by the total number of drivers on the arc; i.e.,

$$tt_a(\boldsymbol{y}) \triangleq t_a \left(1 + b\left(\frac{y_{a_1} + y_{a_2}}{c_a}\right)^4\right), \qquad a \in \mathcal{A}_1 \cup \mathcal{A}_2 \tag{1}$$

where $a_1 = \mathcal{T}_1(\mathcal{T}_0(a))$ and $a_2 = \mathcal{T}_2(\mathcal{T}_0(a))$ are the corresponding arcs for solo drivers and ridesharing drivers, respectively. The values t_a and c_a are constants with respect to the original arc $\mathcal{T}_0(a) \in \mathcal{A}_0$ and b is a common constant. The BPR functions are employed because they are the most common cost functions used in transportation studies; the analysis and solution methods can easily adopt to other functions.

• *Congestion cost for passengers* (experienced by every passenger): Passengers should also experience a congestion cost when they travel. Strictly speaking, the congestion cost is not the same as the travel time, but more as a measure of people's tolerance to travel times. The more the travel time is, the more people have to endure. The passengers, however, are relatively less intolerant to the congestion than the drivers who are traveling on the same (original) arc/path. They do not need to worry about other vehicle-related costs, such as gas cost, especially when it is congested. Therefore the congestion cost of passengers is different from, and most likely less than, that of drivers. In addition this cost may depend on the number of passengers because of the inconvenience of being in a more crowded vehicle. We define this cost as

$$tt_a^{\mathrm{p}}(\boldsymbol{y}) \triangleq t_a \left(1 + b'\left(\frac{y_{a_1} + y_{a_2} + e y_{a_3}}{c_a}\right)^4\right), \qquad a \in \mathcal{A}_3 \tag{2}$$

where $a_j = \mathcal{T}_j(\mathcal{T}_0(a))$ is the corresponding arc of type $j = 1, 2, 3$. Similarly, t_a and c_a are the same as above, and b' and e are positive constants.

• *Inconvenience cost for ridesharing drivers*: Besides the congestion costs, ridesharing drivers will also experience the inconvenience for taking on passengers. Since the congestion costs are the same for both solo and ridesharing drivers, it does not include the cost of picking up, dropping off, or even waiting for passengers. These costs are included in the inconvenience cost, which is given by

$$I_a^{\mathrm{d}}(\boldsymbol{y}) \triangleq \beta^{\mathrm{d}} y_{a_2} + \gamma^{\mathrm{d}} y_{a_3}, \qquad a \in \mathcal{A}_2 \tag{3}$$

where $a_2 = \mathcal{T}_2(\mathcal{T}_0(a)) = a$ and $a_3 = \mathcal{T}_3(\mathcal{T}_0(a))$ are the corresponding arcs for ridesharing drivers and passengers, respectively. The superscript "d" denotes drivers. Both β^{d} and γ^{d} are positive constants.

• *Inconvenience cost for ridesharing passengers*: Similarly, passengers would also experience some inconvenience for taking a ride. The inconvenience cost includes but is not limited to waiting for drivers to pick them up, or possibly having to make a detour together with the driver in order to pick up or drop off other passengers. The cost is defined as

$$I_a^{\mathrm{p}}(\boldsymbol{y}) \triangleq \beta^{\mathrm{p}} y_{a_2} + \gamma^{\mathrm{p}} y_{a_3}, \qquad a \in \mathcal{A}_3 \tag{4}$$

where $a_2 = \mathcal{T}_2(\mathcal{T}_0(a))$ and $a_3 = \mathcal{T}_3(\mathcal{T}_0(a)) = a$ are the corresponding arcs for ridesharing drivers and passengers, respectively. The superscript "p" denotes passengers. Both β^{p} and γ^{p} are positive constants.

• *Ridesharing cost for each passenger* (paying to drivers): In our model, the key point that benefits drivers to participate in ridesharing activities is that they can receive compensation that will cover part of their driving costs. The compensation is in the form of a price paid by each passenger, which is given by

$$R_a^{\mathrm{p}}(\boldsymbol{y}) \triangleq \rho\, t_a - v\, y_{a_2} + w\, y_{a_3}, \qquad a \in \mathcal{A}_3 \tag{5}$$

where $a_2 = \mathcal{T}_2(\mathcal{T}_0(a))$ and $a_3 = \mathcal{T}_3(\mathcal{T}_0(a)) = a$ are the corresponding arcs for ridesharing drivers and passengers, respectively; t_a is the same as in (1) and (2); and ρ, v and w are positive constants.

• *Ridesharing income for each driver* (paid by passengers): Intuitively, the driver's income should equal the sum of the passengers' ridesharing costs (prices) in his/her car. The actual number of passengers in each vehicle is not determined, but belongs to the range $[1, C]$, i.e. at least one passenger and at most C passengers in each vehicle. Hence for simplicity we set the income of each driver to a fixed constant $\alpha \in [1, C]$ times the price paid by each passenger, i.e.

$$R_a^{\mathrm{d}}(\boldsymbol{y}) \triangleq \alpha\, R_a^{\mathrm{p}}(\boldsymbol{y}) = \alpha\,(\,\rho\, t_a - v\, y_{a_2} + w\, y_{a_3}\,), \qquad a \in \mathcal{A}_2. \tag{6}$$

The above cost functions are intended to be as generic as possible, yet still capture the key relations between these costs and the variables. It is the underlying properties of the functions that affect the solutions; the VI/CP methodology is sufficiently broad to handle many function classes.

In sum, each traveler on arc $a \in \mathcal{A}$ experiences a total cost of

$$f_a(\boldsymbol{y}) = \begin{cases} tt_a(\boldsymbol{y}), & a \in \mathcal{A}_1 \\ tt_a(\boldsymbol{y}) + I_a^{\mathrm{d}}(\boldsymbol{y}) - R_a^{\mathrm{d}}(\boldsymbol{y}), & a \in \mathcal{A}_2 \\ tt_a^{\mathrm{p}}(\boldsymbol{y}) + I_a^{\mathrm{p}}(\boldsymbol{y}) + R_a^{\mathrm{p}}(\boldsymbol{y}), & a \in \mathcal{A}_3. \end{cases} \tag{7}$$

Note that the arc cost $f_a(\boldsymbol{y})$ is the same for all OD pairs in $\mathcal{K}$. In this paper, we adopt the additive model for the path costs; that is, the cost $g_p(\boldsymbol{h})$ on a path $p \in \mathcal{P}$ is equal to the sum of the costs on all the arcs traversed by the path:

$$g_p(\boldsymbol{h}) = \sum_{a \in p} f_a(\boldsymbol{y}), \tag{8}$$

where $\boldsymbol{h}$ denotes the path flows that correspond to arc flows $\boldsymbol{y}$.

3.5 A TAP Model with Capacity Constraints

We formulate the model constraints in both arc-based and path-based forms to provide a clear description of the model. The arc formulation is easy for computational purposes and the path formulation is an adaptation of the renowned Wardrop's user equilibrium principle extended to the ridesharing context.

3.5.1 Arc constraints

According to the problem descriptions and assumptions, the constraints of this model can be formulated as below in terms of arc flows.

• Flow decomposition

$$y_a = \sum_{k \in \mathcal{K}} x_a^k, \qquad \forall a \in \mathcal{A} \tag{9}$$

• Flow conservation

$$\sum_{a \in \mathrm{IN}(i)} x_a^k - \sum_{a \in \mathrm{OUT}(i)} x_a^k = 0, \qquad \forall i \in \mathcal{N} \setminus \{o_k, d_k, o_k', d_k'\}, \forall k \in \mathcal{K} \tag{10}$$

• Demand satisfaction

$$\sum_{a \in \mathrm{IN}(d_k) \cup \mathrm{IN}(d_k')} x_a^k - \sum_{a \in \mathrm{OUT}(d_k) \cup \mathrm{OUT}(d_k')} x_a^k = D_k, \qquad \forall k \in \mathcal{K} \tag{11}$$

• Ridesharing capacity

$$y_{a_2} \le y_{a_3} \le C y_{a_2}, \qquad \forall a_0 \in \mathcal{A}_0, a_2 = \mathcal{T}_2(a_0), a_3 = \mathcal{T}_3(a_0) \tag{12}$$

• Nonnegativity

$$x_a^k \ge 0, \qquad \forall a \in \mathcal{A}, \forall k \in \mathcal{K}. \tag{13}$$

Let $\mathcal{Y}$ be the set of feasible arc flows defined by the above constraints; i.e.,

$$\mathcal{Y} \triangleq \{\, \boldsymbol{y} \mid (12) \text{ is satisfied and } \exists\, \boldsymbol{x} \ge 0 \text{ satisfying (9), (10), and (11)} \,\}$$

and let the arc cost functions $f_a(\boldsymbol{y})$ be collected in the vector function $\Phi : \mathcal{Y} \subseteq \mathbb{R}^{|\mathcal{A}|} \to \mathbb{R}^{|\mathcal{A}|}$; thus $\Phi(\boldsymbol{y}) \triangleq (f_a(\boldsymbol{y}))_{a \in \mathcal{A}}$.

Among the above constraints, the one that is most distinguished of the ridesharing paradigm is (12), which in the terminology of [24, 25] is a *side constraint* of the TAP. An alternative way to state this constraint is:

$$\text{lower capacity} = \frac{1}{C} \le \frac{y_{a_2}}{y_{a_3}} \le 1 = \text{ upper capacity}, \quad \text{provided that } y_{a_3} \ne 0.$$

Remark: note that $y_{a_3} = 0$ if and only if $y_{a_2} = 0$; in this case, constraint (12) is trivially satisfied but not very interesting. In the above fractional form, the constraint simply bounds the fraction of ridesharing drivers versus the passengers and stipulates in particular that this fraction must be at

least $1/C$. Associated with the two inequalities in (12) are *admissible multipliers* $\eta^{\pm}_{a_0}$ that satisfy the complementarity conditions:

$$\begin{aligned} 0 \le \eta^{+}_{a_0} \quad &\perp \quad y_{a_3} - y_{a_2} \ge 0 \\ 0 \le \eta^{-}_{a_0} \quad &\perp \quad C\, y_{a_2} - y_{a_3} \ge 0 \end{aligned} \tag{14}$$

where $a_2 = \mathcal{T}_2(a_0)$, $a_3 = \mathcal{T}_3(a_0)$ and the $\perp$ notation denotes perpendicularity, or complementarity between the variables $\eta^{\pm}_{a_0}$ and the slacks of the two inequalities. These complementarity conditions are motivated from the complementary slackness property of linear programming and related to the market clearance in economics. The variables $\eta^{\pm}_{a_0}$ can be interpreted as *compensations* for the limited ridesharing capacities and are positive only if the (variable) upper and lower capacities are binding, respectively.

3.5.2 Path constraints

We have the following relation between the path flow h_p and the arc flow y_a,

$$y_a \;=\; \sum_{p \in \mathcal{P}, a \in \mathcal{A}} \Delta_{ap} h_p, \tag{15}$$

where

$$\Delta_{ap} \triangleq \left\{ \begin{array}{ll} 1, & \text{if path } p \text{ traverses arc } a, \text{ i.e. } a \in p \\ 0, & \text{otherwise,} \end{array} \right\} \quad \forall\, p \in \mathcal{P},\, \forall\, a \in \mathcal{A}.$$

i.e. the amount of flow on arc a is the sum of the flows of all paths passing through the arc. A compact form of (15) is:

$$\boldsymbol{y} = \boldsymbol{\Delta h}, \tag{16}$$

where $\boldsymbol{\Delta}$ is the arc-path incidence matrix with entries Δ_{ap}. Therefore the arc-based constraints (9) through (13) can be written equivalently in terms of path flows h_p as follows.

• Demand satisfaction

$$\sum_{p \in \mathcal{P}_k} h_p \;=\; D_k, \qquad \forall\, k \in \mathcal{K} \tag{17}$$

• Ridesharing capacity

$$\sum_{p \in \mathcal{P}, a_2 \in p} h_p \;\le\; \sum_{p \in \mathcal{P}, a_3 \in p} h_p \;\le\; C \sum_{p \in \mathcal{P}, a_2 \in p} h_p, \qquad \forall\, a_0 \in \mathcal{A}_0,\, a_3 = \mathcal{T}_3\left(a_0\right),\, a_2 = \mathcal{T}_2\left(a_0\right) \tag{18}$$

• Nonnegativity

$$h_p \;\ge\; 0, \qquad \forall\, p \in \mathcal{P}. \tag{19}$$

Let $\mathcal{H}$ be the set of feasible path flows $\boldsymbol{h}$ satisfying (17) through (19). A feasible path flow $\boldsymbol{h}$ *induces* a vector of arc flows $\boldsymbol{y}$ via the definition (16), which can be decomposed into OD-pair based flows $\boldsymbol{x}$ by letting $x^k_a \triangleq \sum_{p \in \mathcal{P}_k, a \in p} h_p$ for every OD pair $k \in \mathcal{K}$ and arc $a \in \mathcal{A}$. It is not difficult to see that such a vector of arc flows $\boldsymbol{x}$ must satisfy the flow conservation (10) and demand requirement (11). Consequently, defining the subset $\widehat{\mathcal{Y}}$ of induced arc flows:

$$\widehat{\mathcal{Y}} \triangleq \left\{\, \boldsymbol{y} \in \mathcal{Y} \mid \exists\, \boldsymbol{h} \in \mathcal{H} \text{ such that } \boldsymbol{y} = \Delta\, \boldsymbol{h} \,\right\},$$

we have $\mathcal{H} = \{ \boldsymbol{h} \geq 0 \,|\, \boldsymbol{\Delta h} \in \widehat{\mathcal{Y}} \}$. Let the path cost functions $g_p(\boldsymbol{h})$ (cf. (8)) be collected in the vector function $\Psi : \mathcal{H} \subseteq \mathbb{R}^{|\mathcal{P}|} \to \mathbb{R}^{|\mathcal{P}|}$; thus, by the additivity condition (8) on these costs, we have

$$\Psi(\boldsymbol{h}) \triangleq (\, g_p(\boldsymbol{h}) \,)_{p \in \mathcal{P}} = \boldsymbol{\Delta}^T \Phi(\boldsymbol{y}) = \boldsymbol{\Delta}^T \Phi(\boldsymbol{\Delta h}). \tag{20}$$

In addition to the costs due to congestion on the links, paths also incur costs due to the ridesharing constraints (18). Specifically, as in [24], define the generalized path costs as a function of the path flow $\boldsymbol{h}$ and multipliers $\boldsymbol{\eta}^{\pm}$ of the ridesharing constraints,

$$\pi_p(\boldsymbol{h}, \boldsymbol{\eta}^{\pm}) \triangleq g_p(\boldsymbol{h}) - \widetilde{\lambda}_p(\boldsymbol{\eta}^{\pm}), \tag{21}$$

where

$$\widetilde{\lambda}_p(\boldsymbol{\eta}^{\pm}) \triangleq \begin{cases} 0 & \text{if } p \cap \mathcal{A}_2 = p \cap \mathcal{A}_3 = \emptyset \\ \displaystyle\sum_{a_2 \in p \cap \mathcal{A}_2} \left(C\, \eta^-_{\mathcal{T}_0(a_2)} - \eta^+_{\mathcal{T}_0(a_2)} \right) & \text{if } p \cap \mathcal{A}_2 \neq \emptyset \\ \displaystyle\sum_{a_3 \in p \cap \mathcal{A}_3} \left(\eta^+_{\mathcal{T}_0(a_3)} - \eta^-_{\mathcal{T}_0(a_3)} \right) & \text{if } p \cap \mathcal{A}_3 \neq \emptyset. \end{cases}$$

3.6 Ridesharing User Equilibrium

One major difference between the ridesharing equilibrium problem and the classical user equilibrium is the ridesharing capacity constraints on arcs, i.e. constraint (12) in the arc formulation, or constraint (18) in the path formulation. In the latter equilibrium, the travel costs of the used paths cannot be reduced. Furthermore, all the used paths of the same OD pair share the same minimum cost. With the capacity constraints, however, the equalization of travel costs is hard to achieve without regards to the compensations induced by these constraints, which are the side constraints, i.e. a set of convex constraints defined on arc flows other than flow conservation or demand requirement. Given the side constraints (18), we formally define a ridesharing user equilibrium based on the classical Wardrop's equilibrium principle, employing the generalized path costs $\pi_p(\boldsymbol{h}, \boldsymbol{\eta}^{\pm})$ defined by (21).

Definition 1. A feasible OD flow $\boldsymbol{h} \in \mathcal{H}$ is a *ridesharing user equilibrium* (RUE) if for every OD pair k, there exists a (sign-unrestricted) minimum generalized travel cost u_k, and for every $a_0 \in \mathcal{A}_0$, there exist admissible multipliers $\eta^{\pm}_{a_0}$ satisfying (14) such that for every path $p \in \mathcal{P}_k$,

$$\begin{aligned} h_p > 0 \;\; &\Rightarrow \;\; \pi_p(\boldsymbol{h}, \boldsymbol{\eta}^{\pm}) = u_k \\ h_p = 0 \;\; &\Rightarrow \;\; \pi_p(\boldsymbol{h}, \boldsymbol{\eta}^{\pm}) \geq u_k. \end{aligned} \tag{22}$$

In words, the generalized costs of all used paths (i.e., those with positive flows) joining the same OD pair must be equal and are not greater than the generalized costs of the unused paths joining the same OD pair. □

Substituting the function $\pi_p(\boldsymbol{h}, \boldsymbol{\eta}^{\pm})$ from (21) and the properties of the multipliers $\eta^{\pm}_{a_0}$ from (14),

we deduce the following MiCP formulation of a RUE:

$$0 \le h_p \quad \perp \quad g_p(\boldsymbol{h}) - \widetilde{\lambda}_p(\boldsymbol{\eta}^{\pm}) - \mu_k \ge 0, \qquad \forall k \in \mathcal{K}, \forall p \in \mathcal{P}_k \tag{23}$$

$$0 \le \eta_a^+ \quad \perp \quad \sum_{p \in \mathcal{P}, \mathcal{T}_3(a) \in p} h_p - \sum_{p \in \mathcal{P}, \mathcal{T}_2(a) \in p} h_p \ge 0, \qquad \forall a \in \mathcal{A}_0 \tag{24}$$

$$0 \le \eta_a^- \quad \perp \quad C \sum_{p \in \mathcal{P}, \mathcal{T}_2(a) \in p} h_p - \sum_{p \in \mathcal{P}, \mathcal{T}_3(a) \in p} h_p \ge 0, \qquad \forall a \in \mathcal{A}_0 \tag{25}$$

$$\mu_k \text{ free} \quad \text{and} \quad \sum_{p \in \mathcal{P}_k} h_p = D_k, \qquad \forall k \in \mathcal{K}. \tag{26}$$

3.7 Saturation

If a path contains no arcs in $\mathcal{A}_2$ and $\mathcal{A}_3$, i.e., if the path is for solo drivers only, then ridesharing capacity is a non-issue for this path. Nevertheless, if the path contains one of these types of arcs, then the upper/lower ridesharing capacity, when it is reached, adds/subtracts a positive cost to the standard travel cost of the path.

Definition 2. Let $\boldsymbol{y}$ and $\boldsymbol{h}$ be arc- and path-flow vectors related by $\boldsymbol{y} = \boldsymbol{\Delta h}$. We say that

• an *arc* $a_2 \in \mathcal{A}_2$ (or $a_3 \in \mathcal{A}_3$) is *saturated above* if $y_{a_2} = y_{a_3}$ (or $y_{a_3} = C y_{a_2}$), i.e. the flow y_{a_2} (or y_{a_3}) reaches its upper bound;

• an *arc* $a_2 \in \mathcal{A}_2$ (or $a_3 \in \mathcal{A}_3$) is *saturated below* if $y_{a_2} = \frac{1}{C} y_{a_3}$ (or $y_{a_3} = y_{a_2}$), i.e. the flow y_{a_2} (or y_{a_3}) reaches its lower bound;

• an *arc* $a \in \mathcal{A}_2 \cup \mathcal{A}_3$ is *saturated* if it is either saturated above or saturated below;

• a *path* p is *saturated above* if it contains at least one saturated-above arc and no saturated-below arc;

• a *path* p is *saturated below* if it contains at least one saturated-below arc and no saturated-above arc;

• a *path* p is *saturated* if it is either saturated above or saturated below (and not both).

• a *path* p is *unchangeable* if it contains both saturated-above and saturated-below arcs. □

Note that according to Definition 2, an arc $a_1 \in \mathcal{A}_1$ can never be saturated since it does not have an upper or lower bound. Also, whenever an arc $a_2 \in \mathcal{A}_2$ is saturated above (or below), there also exists an arc $a_3 \in \mathcal{A}_3$ on a different path that is saturated below (or above). Lastly, a path is changeable if either it contains no saturated-above arcs or it contains no saturated-below arc. The generalized equilibrium cost of such a path is not necessarily equal to the minimum OD cost; see derivations below.

Employing the saturation properties, the compensation costs on the paths due to the ridesharing capacity can be simplified as follows, yielding several consequences relating the travel costs $g_p(\boldsymbol{h})$ on used paths, the minimum generalized OD costs u_k, and the arc compensations $\eta_a^{\pm}$ of a RUE triple $(\boldsymbol{h}, \boldsymbol{\eta}^{\pm}, \boldsymbol{u})$.

(A) If path p contains no saturated-below arcs, then

$$\widetilde{\lambda}_p(\boldsymbol{\eta}^{\pm}) \triangleq \begin{cases} 0 & \text{if } p \cap \mathcal{A}_2 = p \cap \mathcal{A}_3 = \emptyset \\ -\sum_{a_2 \in p \cap \mathcal{A}_2} \eta^{+}_{\mathcal{T}_0(a_2)} & \text{if } p \cap \mathcal{A}_2 \neq \emptyset \\ -\sum_{a_3 \in p \cap \mathcal{A}_3} \eta^{-}_{\mathcal{T}_0(a_3)} & \text{if } p \cap \mathcal{A}_3 \neq \emptyset; \end{cases}$$

thus $\widetilde{\lambda}_p(\boldsymbol{\eta}^{\pm}) \leq 0$; in this case:

$$h_p > 0 \;\Rightarrow\; g_p(\boldsymbol{h}) = u_k + \widetilde{\lambda}_p(\boldsymbol{\eta}^{\pm}) \leq u_k;$$

in particular, if a used path is saturated above, then its travel cost is not greater than the minimum generalized OD cost u_k.

(B) If path p contains no saturated-above arcs, then

$$\widetilde{\lambda}_p(\boldsymbol{\eta}^{\pm}) \triangleq \begin{cases} 0 & \text{if } p \cap \mathcal{A}_2 = p \cap \mathcal{A}_3 = \emptyset \\ \sum_{a_2 \in p \cap \mathcal{A}_2} C\, \eta^{-}_{\mathcal{T}_0(a_2)} & \text{if } p \cap \mathcal{A}_2 \neq \emptyset \\ \sum_{a_3 \in p \cap \mathcal{A}_3} \eta^{+}_{\mathcal{T}_0(a_3)} & \text{if } p \cap \mathcal{A}_3 \neq \emptyset; \end{cases}$$

thus $\widetilde{\lambda}_p(\boldsymbol{\eta}^{\pm}) \geq 0$. In this case, we have

$$g_p(\boldsymbol{h}) \geq u_k + \widetilde{\lambda}_p(\boldsymbol{\eta}^{\pm}) \geq u_k.$$

(C) If a used path p contains no saturated-above and no saturated-below arcs, then $g_p(\boldsymbol{h}) = u_k$ and $\eta^{\pm}_{\mathcal{T}_0(a)} = 0$ for all $a \in p \cap (\mathcal{A}_2 \cup \mathcal{A}_3)$.

(D) If a used path p has travel cost $g_p(\boldsymbol{h}) < (>) u_k$, then the path is either unchangeable or saturated above (below). [Proof: Suppose $g_p(\boldsymbol{h}) < u_k$; by (B), p must contain a saturated-above arc. If p also contains a saturated-below arc, then it is unchangeable; otherwise it is saturated above.]

4 Existence and Uniqueness of RUE

While an MiCP formulation of the RUE facilitates the solution of the problem by existing software (see the next section), an equivalent formulation as a variational inequality allows us to establish the existence and uniqueness of a solution to the model. Specifically, we have the following result that summarizes the VI/CP formulation and formally asserts the existence of a RUE. The proof is an immediate consequence of well-known VI/CP results [14] and is omitted.

Theorem 1. *Let $\boldsymbol{h} \in \mathcal{H}$ be a feasible path flow and $\boldsymbol{y}$ a feasible arc flow induced by $\boldsymbol{h}$. The following statements hold.*

(a) *$\boldsymbol{h}$ is a RUE;*

(b) *there exists $\boldsymbol{\eta}^{\pm}$ satisfying (14) and $\boldsymbol{u}$ such that $(\boldsymbol{h}, \boldsymbol{\eta}^{\pm}, \boldsymbol{u})$ satisfies the MiCP (23)–(26).*

(c) $\boldsymbol{h}$ *is a solution of the VI* $(\mathcal{H}, \Psi)$*;*

(c) $\boldsymbol{y}$ *is a solution of the VI* $(\widehat{\mathcal{Y}}, \Phi)$*;*

(d) *If* Ψ *is continuous, then a RUE exists.* □

Part (d) of the above theorem yields the existence of a ridesharing user equilibrium. In general, the path flows of such an equilibrium are not unique; i.e., the VI $(\mathcal{H}, \Psi)$ does not necessarily have a unique solution. Nevertheless, under the assumptions on the model parameter as specified in Theorem 2 below, there is a unique vector of induced arc flows among all ridesharing user equilibria. The proof of this theorem is based on the strict monotonicity of the mapping Φ under certain conditions on the model parameters. Under this monotonicity property, the arc flow VI $(\mathcal{Y}, \Phi)$ has at most one solution by [14, Theorem 2.3.3(a)], which is necessarily a ridesharing user equilibrium. Since such an equilibrium exists, the uniqueness of the induced arc flows follows readily. In turn, the strict monotonicity of Φ is proved by verifying the positive definiteness of the Jacobian matrix $J\Phi(\boldsymbol{y})$ for all $\boldsymbol{y} \in \mathcal{Y}$. The calculation of the latter matrix is straightforward; details can be found in [36]. Roughly, the matrix $J\Phi(\boldsymbol{y})$ is block diagonal with $3 \times |\mathcal{A}_0|$ diagonal blocks, each of which corresponds to an arc $a_0 \in \mathcal{A}_0$ and is given by

$$\begin{bmatrix} \dfrac{\partial f_{a_1}(\boldsymbol{y})}{\partial y_{a_1}} & \dfrac{\partial f_{a_1}(\boldsymbol{y})}{\partial y_{a_2}} & \dfrac{\partial f_{a_1}(\boldsymbol{y})}{\partial y_{a_3}} \\ \dfrac{\partial f_{a_2}(\boldsymbol{y})}{\partial y_{a_1}} & \dfrac{\partial f_{a_2}(\boldsymbol{y})}{\partial y_{a_2}} & \dfrac{\partial f_{a_2}(\boldsymbol{y})}{\partial y_{a_3}} \\ \dfrac{\partial f_{a_3}(\boldsymbol{y})}{\partial y_{a_1}} & \dfrac{\partial f_{a_3}(\boldsymbol{y})}{\partial y_{a_1}} & \dfrac{\partial f_{a_3}(\boldsymbol{y})}{\partial y_{a_1}} \end{bmatrix}$$

$$= \begin{bmatrix} \dfrac{\partial tt_{a_1}(\boldsymbol{y})}{\partial y_{a_1}} & \dfrac{\partial tt_{a_1}(\boldsymbol{y})}{\partial y_{a_2}} & \dfrac{\partial tt_{a_1}(\boldsymbol{y})}{\partial y_{a_3}} \\ \dfrac{\partial tt_{a_2}(\boldsymbol{y})}{\partial y_{a_1}} & \dfrac{\partial tt_{a_2}(\boldsymbol{y})}{\partial y_{a_2}} & \dfrac{\partial tt_{a_2}(\boldsymbol{y})}{\partial y_{a_3}} \\ \dfrac{\partial tt^{\mathrm{p}}_{a_3}(\boldsymbol{y})}{\partial y_{a_1}} & \dfrac{\partial tt^{\mathrm{p}}_{a_3}(\boldsymbol{y})}{\partial y_{a_2}} & \dfrac{\partial tt^{\mathrm{p}}_{a_3}(\boldsymbol{y})}{\partial y_{a_3}} \end{bmatrix} + \begin{bmatrix} 0 & 0 & 0 \\ 0 & \dfrac{\partial \left(I^{\mathrm{d}}_{a_2}(\boldsymbol{y}) - R^{\mathrm{d}}_{a_2}(\boldsymbol{y}) \right)}{\partial y_{a_2}} & \dfrac{\partial \left(I^{\mathrm{d}}_{a_2}(\boldsymbol{y}) - R^{\mathrm{d}}_{a_2}(\boldsymbol{y}) \right)}{\partial y_{a_3}} \\ 0 & \dfrac{\partial \left(I^{\mathrm{p}}_{a_3}(\boldsymbol{y}) + R^{\mathrm{p}}_{a_3}(\boldsymbol{y}) \right)}{\partial y_{a_2}} & \dfrac{\partial \left(I^{\mathrm{p}}_{a_3}(\boldsymbol{y}) + R^{\mathrm{p}}_{a_3}(\boldsymbol{y}) \right)}{\partial y_{a_3}} \end{bmatrix}$$

where $a_i = \mathcal{T}_i(a_0)$ for $i = 1, 2, 3$. The first inequality in (27) below is necessary and sufficient for (the symmetric part of) the matrix

$$\begin{bmatrix} \dfrac{\partial \left(I^{\mathrm{d}}_{a_2}(\boldsymbol{y}) - R^{\mathrm{d}}_{a_2}(\boldsymbol{y}) \right)}{\partial y_{a_2}} & \dfrac{\partial \left(I^{\mathrm{d}}_{a_2}(\boldsymbol{y}) - R^{\mathrm{d}}_{a_2}(\boldsymbol{y}) \right)}{\partial y_{a_3}} \\ \dfrac{\partial \left(I^{\mathrm{p}}_{a_3}(\boldsymbol{y}) + R^{\mathrm{p}}_{a_3}(\boldsymbol{y}) \right)}{\partial y_{a_2}} & \dfrac{\partial \left(I^{\mathrm{d}}_{a_p}(\boldsymbol{y}) + R^{\mathrm{p}}_{a_3}(\boldsymbol{y}) \right)}{\partial y_{a_3}} \end{bmatrix}$$

to be positive semidefinite.

Theorem 2. *Suppose that the parameters of the cost functions as specified in Subsection 3.4 satisfy,*

$$\begin{array}{lll} 4(\,\beta^{\,\mathrm{d}} + \alpha v\,)\,(\,\gamma^{\,\mathrm{p}} + w\,) - (\,\gamma^{\,\mathrm{d}} - \alpha w + \beta^{\,\mathrm{p}} - v\,)^2 & \geq & 0, \\ \textit{and} \quad 4\,e\,b - b'\,(\,1 + e\,C\,)^3 & \geq & 0, \end{array} \tag{27}$$

with at least one of the above two inequalities holding strictly, then there exists a unique ridesharing arc-flow equilibrium. □

The conditions above establish bounds on the rate of change of the cost functions for ridesharing drivers and passengers. The first inequality in (27) holds if

$$\beta^{\,\mathrm{d}} + \alpha v \;=\; \frac{\partial \left(I^{\mathrm{d}}_{a_2}(\boldsymbol{y}) - R^{\mathrm{d}}_{a_2}(\boldsymbol{y}) \right)}{\partial y_{a_2}}$$

$$> \; \tfrac{1}{2} \left[\left| \gamma^{\,\mathrm{d}} - \alpha w \right| + \left| \beta^{\,\mathrm{p}} - v \right| \right] \;=\; \tfrac{1}{2} \left[\left| \frac{\partial \left(I^{\mathrm{d}}_{a_2}(\boldsymbol{y}) - R^{\mathrm{d}}_{a_2}(\boldsymbol{y}) \right)}{\partial y_{a_3}} \right| + \left| \frac{\partial \left(I^{\mathrm{p}}_{a_3}(\boldsymbol{y}) + R^{\mathrm{p}}_{a_3}(\boldsymbol{y}) \right)}{\partial y_{a_2}} \right| \right]$$

and

$$\gamma^{\,\mathrm{p}} + w \;=\; \frac{\partial \left(I^{\mathrm{p}}_{a_3}(\boldsymbol{y}) + R^{\mathrm{p}}_{a_3}(\boldsymbol{y}) \right)}{\partial y_{a_3}} \;>\; \tfrac{1}{2} \left[\left| \frac{\partial \left(I^{\mathrm{d}}_{a_2}(\boldsymbol{y}) - R^{\mathrm{d}}_{a_2}(\boldsymbol{y}) \right)}{\partial y_{a_3}} \right| + \left| \frac{\partial \left(I^{\mathrm{p}}_{a_3}(\boldsymbol{y}) + R^{\mathrm{p}}_{a_3}(\boldsymbol{y}) \right)}{\partial y_{a_2}} \right| \right];$$

these inequalities have the interpretation that variations of driver (passenger) cost due to changes in drivers (passengers) dominate the corresponding cross rates of changes.

The second condition in (27) bounds rates of change of the travel time component of the cost (either $tt_a(\boldsymbol{y})$ or $tt^{\mathrm{p}}_a(\boldsymbol{y})$). This condition can be rewritten as $\dfrac{b}{b'} \geq \dfrac{(1+eC)^3}{4e}$. The left-hand ratio can be viewed as some measure of the savings in the travel time multipliers for a traveler to become a passenger instead of a driver while the right-hand fraction can be viewed as the extra congestion factor for someone to become a passenger. Under this condition, it can be shown that $\dfrac{\partial tt_a(\boldsymbol{y})/\partial y_{a_2}}{\partial tt^{\mathrm{p}}_a(\boldsymbol{y})/\partial y_{a_3}} \geq \dfrac{1}{4e^2}$, which provides a lower bound on the rate of change of the travel time component of ridesharing drivers with respect to the rate of change of the travel time component of passengers. The upshot of Theorem 2 is that under these conditions on the variations of driver (passenger) costs due to the change of roles among the drivers and passengers and on the relative savings in the travel time of the ridesharing drivers, the variational model of ridesharing equilibrium admits a unique solution whose computation and sensitivity analysis are the topics of the next section.

5 Computational Results

To facilitate the numerical computation of the RUE, we introduce the MiCP formulation in terms of the OD-based arc flows x^k_a. This formulation follows readily from the substitution (9) of the flow variables y_a in terms of x^k_k into the VI $(\widehat{\mathcal{Y}}, \Phi)$, yielding a corresponding VI in the $\boldsymbol{x}$-variables. The equivalent complementarity formulation of the latter VI is:

$$\begin{aligned}
0 \;\leq\; x^k_a \quad &\perp \quad f_a(\boldsymbol{\Omega x}) + \omega^+_a \eta^+_{\mathcal{T}_0(a)} + \omega^-_a \eta^-_{\mathcal{T}_0(a)} - \mu^k_i + \mu^k_j \geq 0, \quad \forall\, a = (i,j) \in \mathcal{A} \,\text{and}\, \forall\, k \in \mathcal{K} \\
0 \;\leq\; \eta^+_a \quad &\perp \quad \sum_{k \in \mathcal{K}} x^k_{a_3} - \sum_{k \in \mathcal{K}} x^k_{a_2} \;\geq\; 0, \quad \forall\, a \in \mathcal{A}_0,\, a_2 = \mathcal{T}_2(a),\, \text{and}\, a_3 \;=\; \mathcal{T}_3(a) \\
0 \;\leq\; \eta^-_a \quad &\perp \quad C \sum_{k \in \mathcal{K}} x^k_{a_2} - \sum_{k \in \mathcal{K}} x^k_{a_3} \;\geq\; 0, \quad \forall\, a \in \mathcal{A}_0,\, a_2 = \mathcal{T}_2(a),\, \text{and}\, a_3 = \mathcal{T}_3(a) \\
\mu^k_i \;\text{free}, \quad \text{and} \quad & \sum_{a \in \mathrm{IN}(i)} x^k_a - \sum_{a \in \mathrm{OUT}(i)} x^k_a \;=\; 0, \quad \forall\, i \in \mathcal{N} \setminus \{o_k, d_k, o'_k, d'_k\},\, \text{and}\, \forall\, k \in \mathcal{K} \\
\mu^k_d \;\text{free}, \quad \text{and} \quad & \sum_{a \in \mathrm{IN}(d_k) \cup \mathrm{IN}(d'_k)} x^k_a - D_k \;=\; 0, \quad \forall\, k \in \mathcal{K},
\end{aligned}$$

where ω_a^+ and ω_a^- are constant coefficients given by

$$\omega_a^+ \triangleq \begin{cases} 0 & \text{if } a \in \mathcal{A}_1 \\ 1 & \text{if } a \in \mathcal{A}_2 \\ -1 & \text{if } a \in \mathcal{A}_3 \end{cases} \quad \text{and} \quad \omega_a^- \triangleq \begin{cases} 0 & \text{if } a \in \mathcal{A}_1 \\ -C & \text{if } a \in \mathcal{A}_2 \\ 1 & \text{if } a \in \mathcal{A}_3 \end{cases}$$

and $\boldsymbol{\Omega}\boldsymbol{x} = \boldsymbol{y}$ is the compact form of $y_a = \sum_{k \in \mathcal{K}} x_a^k$; more specifically, $\boldsymbol{\Omega} \triangleq \left[\boldsymbol{I}_1, \ldots, \boldsymbol{I}_{|\mathcal{K}|}\right] \in \mathbb{R}^{|\mathcal{A}| \times |\mathcal{A}||\mathcal{K}|}$ and each $\boldsymbol{I}_k$ is the identity matrix of order $|\mathcal{A}| \times |\mathcal{A}|$.

The numerical results reported below are obtained by applying the KNITRO solver on the NEOS server [10, 19, 13] to the above MiCP. These results pertain to different test cases.

5.1 Three-node Network

Consider the following example where the original graph has 3 nodes and 6 arcs, $\mathcal{N}_0 = \{1, 2, 3\}$, and $\mathcal{A}_0 = \{(1,2), (2,1), (1,3), (3,1), (2,3), (3,2)\}$. The arc capacities are given by $c_1 = c_2 = 259$, $c_3 = c_4 = 234$, and $c_5 = c_6 = 149$. The set of OD pairs includes all 6 trips, i.e.,

$$\mathcal{K} = \{(1,2), (2,1), (1,3), (3,1), (2,3), (3,2)\}.$$

For each trip the demand is 100, i.e. there are 100 people traveling from node 1 to node 2, some (or none or all) of them can be solo drivers and some can be ridesharing drivers or passengers.

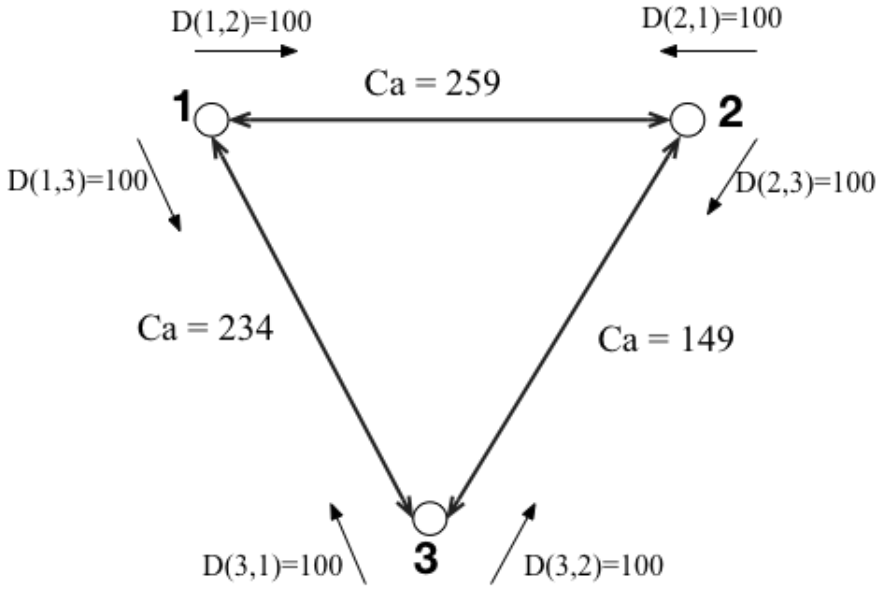

Figure 2: Example with trips and arc capacities for three-node network

Other parameter settings are given in Table 1. All arc parameters are based on the original network, i.e. $a \in \mathcal{A}_0 = \{1, \ldots, 6\}$ in this case. The duplicated arcs have the same parameter settings as the original arcs. It can also be checked that the parameters in Table 1 satisfy both inequalities in (27) strictly. Hence there exists a unique arc-flow RUE.

Table 1: Parameter settings for three-node network

Description	Constants	Values
free flow time	$t_a (a = 1, \ldots, 6)$	$6, 6, 4, 4, 5, 5$
arc capacity (threshold)	$c_a (a = 1, \ldots, 6)$	$259, 259, 234, 234, 149, 149$
congestion coefficients	b, b', e	$0.15,\ 0.015,\ 0.3$
inconvenience coefficients	$\beta^{\mathrm{d}}, \beta^{\mathrm{p}}$	0.1
inconvenience coefficients	γ^{d}, γ^{p}	0.01
price coefficients	ρ, v, w	$0.5,\ 0.2,\ 0.1$
vehicle capacity	α, C	$2,\ 4$
demand	$D_k (k = 1, \ldots, 6)$	100

Note that we set $b' < b$ making the congestion cost of passengers less than that of the drivers. We also set $e < 1$, since the contribution of passengers to the congestion cost is considerably less than that of drivers. As for the inconvenience costs, we set $\beta^{\mathrm{d}} \geq \gamma^{\mathrm{d}}$, under the assumption that drivers contribute more on the inconvenience cost of each driver than passengers. In other words, we assume that the inconvenience cost for drivers of adding one passenger is less than adding one ridesharing driver. Similarly, we set $\beta^{\mathrm{p}} \geq \gamma^{\mathrm{p}}$, assuming that drivers contribute more on the inconvenience cost of each passenger. β^{p} (or γ^{p}) could be either the same or different from β^{d} (or γ^{d}). Finally, we set $v > w$ under the assumption that adding one passenger will contribute less to the ridesharing price than adding one driver. With these settings, the results are shown in Table 2, where only the nonzero x_a^k are listed.

Table 2: Computational results for $\boldsymbol{x}$ for the three-node network

$(k,\ a)$	$x^k_{a_1}$	$(k,\ a)$	$x^k_{a_2}$	$(k,\ a)$	$x^k_{a_3}$
$(1,\ \mathcal{T}_1(1))$	81.1756	$(1,\ \mathcal{T}_2(1))$	9.4122	$(1,\ \mathcal{T}_3(1))$	9.4122
$(2,\ \mathcal{T}_1(3))$	87.4147	$(2,\ \mathcal{T}_2(3))$	6.2927	$(2,\ \mathcal{T}_3(3))$	6.2927
$(3,\ \mathcal{T}_1(2))$	81.1756	$(3,\ \mathcal{T}_2(2))$	9.4122	$(3,\ \mathcal{T}_3(2))$	9.4122
$(4,\ \mathcal{T}_1(5))$	83.7752	$(4,\ \mathcal{T}_2(5))$	8.1124	$(4,\ \mathcal{T}_3(5))$	8.1124
$(5,\ \mathcal{T}_1(4))$	87.4147	$(5,\ \mathcal{T}_2(4))$	6.2927	$(5,\ \mathcal{T}_3(4))$	6.2927
$(6,\ \mathcal{T}_1(6))$	83.7752	$(6,\ \mathcal{T}_2(6))$	8.1124	$(6,\ \mathcal{T}_3(6))$	8.1124

The values of the multipliers are $\eta_1^+ = \eta_2^+ = 3.08221$, $\eta_3^+ = \eta_4^+ = 2.04928$, $\eta_5^+ = \eta_6^+ = 2.48516$, and $\eta_a^- = 0$, for all $a \in \mathcal{A}_0 = \{1, \ldots, 6\}$. The values of $\boldsymbol{\mu}$ are omitted. Note that for each arc $a \in \mathcal{A}$ the flow on a comes from *only one* OD pair, therefore y_a equals to the corresponding x_a^k with the same a. The values of y_a, $f_a(\boldsymbol{y})$ and $\widetilde{\Theta}_{a,k}(\boldsymbol{x})$ are given in Table 3, where

$$\widetilde{\Theta}_{a,k}(\boldsymbol{x}) \triangleq f_a(\boldsymbol{\Omega x}) + \omega_a^+ \eta^+_{\mathcal{T}_0(a)} + \omega_a^- \eta^-_{\mathcal{T}_0(a)} - \mu_i^k + \mu_j^k, \quad \forall a = (i,j) \in \mathcal{A}, \forall k \in \mathcal{K}$$

Note that we only care about those $\widetilde{\Theta}_{a,k}(\boldsymbol{x})$ for which x_a^k is nonzero.

Since every path consists of *only one* arc, the path cost equals to the corresponding arc cost. For each OD pair, the generalized cost of each path, which is calculated by $f_a(\boldsymbol{\Omega x}) + \omega_a^+ \eta^+_{\mathcal{T}_0(a)} + \omega_a^- \eta^-_{\mathcal{T}_0(a)}$, equals to the same constant. For example, when $k = 1$, there are altogether three paths, using arcs $a = 1, 2, 3$, respectively. This means that, 81.1756 out of the 100 travelers are driving alone from node 1 to node 2, while 9.4122 are taking on passengers and the rest 9.4122 are traveling as passengers. The travel costs experienced by each traveler for the different travel modes are $f_2(\boldsymbol{y}) + \eta_1^+ - C\eta_1^- = f_3(\boldsymbol{y}) - \eta_1^+ + \eta_1^- = f_1(\boldsymbol{y}) = 6.0134$.

Table 3: Computational results for $\boldsymbol{y}$ and the costs for the three-node network

a	y_a	$f_a(\boldsymbol{y})$	$\widetilde{\Theta}_{a,k}(\boldsymbol{x})$	a	y_a	$f_a(\boldsymbol{y})$	$\widetilde{\Theta}_{a,k}(\boldsymbol{x})$
$\mathcal{T}_1(1)$	81.1756	6.0134	0.0000	$\mathcal{T}_1(4)$	87.4147	4.0153	0.0000
$\mathcal{T}_2(1)$	9.4122	2.9312	0.0000	$\mathcal{T}_2(4)$	6.2927	1.9660	0.0000
$\mathcal{T}_3(1)$	9.4122	9.0956	0.0000	$\mathcal{T}_3(4)$	6.2927	6.0646	0.0000
$\mathcal{T}_1(2)$	81.1756	6.0134	0.0000	$\mathcal{T}_1(5)$	83.7752	5.1080	0.0000
$\mathcal{T}_2(2)$	9.4122	2.9312	0.0000	$\mathcal{T}_2(5)$	8.1124	2.6228	0.0000
$\mathcal{T}_3(2)$	9.4122	9.0956	0.0000	$\mathcal{T}_3(5)$	8.1124	7.5931	0.0000
$\mathcal{T}_1(3)$	87.4147	4.0153	0.0000	$\mathcal{T}_1(6)$	83.7752	5.1080	0.0000
$\mathcal{T}_2(3)$	6.2927	1.9660	0.0000	$\mathcal{T}_2(6)$	8.1124	2.6228	0.0000
$\mathcal{T}_3(3)$	6.2927	6.0646	0.0000	$\mathcal{T}_3(6)$	8.1124	7.5931	0.0000

Under the ridesharing user equilibrium, the generalized costs experienced by each traveler of the same OD pair are the same, although their travel costs $f_a(\boldsymbol{y})$ may vary. Moreover, it can be seen that all paths are saturated from the perspective of the ridesharing drivers. Therefore even though ridesharing drivers are experiencing the least travel costs, others cannot switch to become a ridesharing driver. From the perspective of passengers, their travel costs are the highest. But since their path is saturated below, people cannot leave this path for cheaper-cost paths. It can also be calculated from Table 3 that on average, the proportions of solo drivers, ridesharing drivers and passengers on each arc are, respectively, 84.12% : 7.94% : 7.94%.

5.2 The Braess Network

One interesting test case for the traffic equilibrium problems is the Braess network (see Figure 3). In the original graph, $\mathcal{N}_0 = \{1, 2, 3, 4\}$, $\mathcal{A}_0 = \{(1, 3), (1, 4), (3, 2), (3, 4), (4, 2)\}$ (for simplicity, rewrite $\mathcal{A}_0 = \{1, \ldots, 5\}$), and there is only one OD pair $\mathcal{K} = \{(1, 2)\}$ with demand $D(1, 2) = 6$.

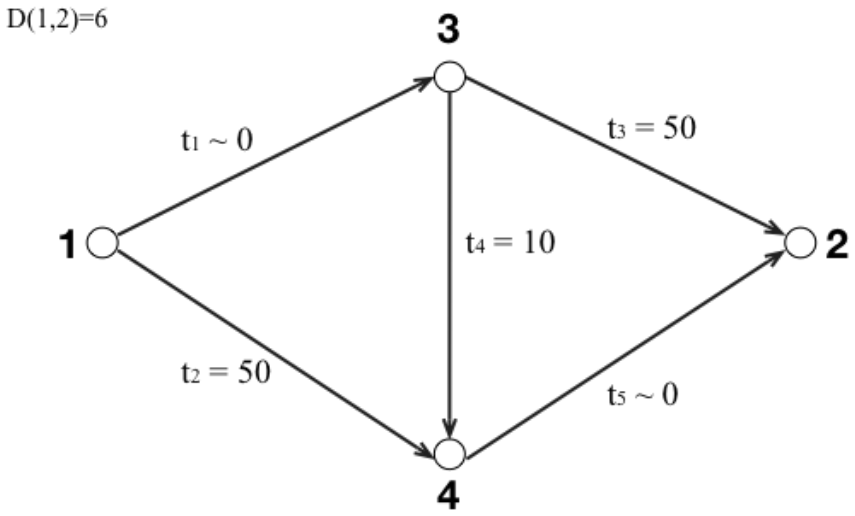

Figure 3: Example with trips and free flow travel times for Braess

The free flow time is also labeled by each arc in Figure 3, i.e. $t_1 = t_5 = 0.00000001 \approx 0$, $t_2 = t_3 = 50$ and $t_4 = 10$. Other parameter settings are given in Table 4. For the Braess network the exponent in the BPR function is set to 1, $f_a(\boldsymbol{y}) = t_a \left[1 + b\left(\frac{y_{a_1} + y_{a_2}}{c_a}\right)\right]$ for the drivers and $f_a(\boldsymbol{y}) = t_a \left[1 + b'\left(\frac{y_{a_1} + y_{a_2} + e y_{a_3}}{c_a}\right)\right]$ for the passengers.

Table 4: Parameter settings for the Braess network

Description	Constants	Values
free flow time	$t_a (a = 1, \ldots, 5)$	0, 50, 50, 10, 0
arc capacity (threshold)	$c_a (a = 1, \ldots, 5)$	1
congestion coefficients	$b_a (a = 1, \ldots, 5)$	$10^9, 0.02, 0.02, 0.1, 10^9$
congestion coefficients	b'_a, e	$0.1 b_a$, 0.3
inconvenience coefficients	β^{d}, β^{p}	0.1
inconvenience coefficients	γ^{d}, γ^{p}	0.01
price coefficients	ρ, v, w	0.5, 0.2, 0.1
vehicle capacity	α, C	2, 4
demand	D_1 $(1 \to 2)$	6

The Braess network leads to some interesting paradoxes in network flows. Consider the simplest case: suppose all travelers are solo drivers. Every traveler will observe a travel cost of 10 on path "$1 \to 3 \to 4 \to 2$" before traveling. Since each of them acts selfishly, all of them will travel on that path. As a result, the cost would increase to 60 due to congestion. If they cooperate, they could reduce the travel cost to 50 for each of them. Now consider our ridesharing case, where travelers may choose to be a solo driver, a ridesharing driver or a passenger. Given the above parameter settings for the network, the computational results are shown in Table 5. Note that there is only one OD pair $(1 \to 2)$, hence all y_a equal x_a.

Table 5: Computational results for the Braess network

a	$x_a = y_a$	$f_a(\boldsymbol{y})$	$\widetilde{\Theta}_{a,k}(\boldsymbol{x})$
$\mathcal{T}_1(1)$	0.0	12.000	X
$\mathcal{T}_2(1)$	1.2	11.688	0.000
$\mathcal{T}_3(1)$	4.8	3.048	0.000
$\mathcal{T}_1(2)$	0.0	50.000	X
$\mathcal{T}_2(2)$	0.0	0.000	X
$\mathcal{T}_3(2)$	0.0	75.000	X
$\mathcal{T}_1(3)$	0.0	50.000	X
$\mathcal{T}_2(3)$	0.0	0.000	X
$\mathcal{T}_3(3)$	0.0	75.000	X
$\mathcal{T}_1(4)$	0.0	11.200	X
$\mathcal{T}_2(4)$	1.2	0.888	0.000
$\mathcal{T}_3(4)$	4.8	15.672	0.000
$\mathcal{T}_1(5)$	0.0	12.000	X
$\mathcal{T}_2(5)$	1.2	11.688	0.000
$\mathcal{T}_3(5)$	4.8	3.048	0.000

Table 5 shows us that the average proportion of solo driver, ridesharing driver and passenger on each arc is 0% : 20% : 80%. The values of $\widetilde{\Theta}_{a,k}(\boldsymbol{x})$ for $x_a \approx 0$ (as obtained from the solver) have been labeled by "X", since these values are of no interest. From Table 5 we can tell that all travelers are choosing the path "$1 \to 3 \to 4 \to 2$". No traveler is a solo driver. 1.2 out of 6 of them choose to be a ridesharing driver and the remaining 4.8 of them choose to be passengers. The costs of all the paths are given in Table 6.

Table 6: The path costs for the Braess network

path	$1 \to 3 \to 4 \to 2$	$1 \to 3 \to 2$	$1 \to 4 \to 2$
solo driver	35.2	62.0	62.0
ridesharing driver	24.3	11.7	11.7
passenger	21.8	78.0	78.0

It can be easily seen that, for the used path "$1 \to 3 \to 4 \to 2$", the cost of solo drivers (35.2) is the highest, and thus no one would like to drive alone. The cost of passengers (21.8) is the lowest. But since there is a capacity constraint for each vehicle, i.e. each driver can take on at most $C = 4$ passengers. No more travelers can switch to be a passenger. This is exactly the case in the ridesharing user equilibrium, where the costs of the other used paths cannot be reduced since the least cost path is saturated with $y_{a_3} = Cy_{a_2}$. For the other unused paths, the costs of both solo drivers and passengers are much greater than the used paths. Therefore even though the ridesharing drivers may have an even lower cost (11.7) than the current used path, these unused paths are saturated for ridesharing drivers. Since there are zero passengers on these paths, people cannot switch to be a ridesharing driver given the bound $0 \le y_{a_2} \le y_{a_3} = 0$. In other words, since there are no passengers on the unused paths, a driver that selects that path would be a solo driver and experience a high cost (62.0), making it an unattractive choice.

5.3 The Sioux-Falls Network

Up to now we have seen from the first two test cases that both the lower bounds and the upper bounds in (12) or (18) have been reached. These cases are relatively small and simple. In what follows, we will study the Sioux-Falls network and see how ridesharing drivers will take on passengers from other OD pairs. The data set of Sioux-Falls was downloaded from the website called "Transportation Network Test Problems" (`http://www.bgu.ac.il/~bargera/tntp/`.) The original data contains a network with 24 nodes and 76 arcs. The set of OD pairs covers almost all 24×23 combinations of node pairs—there are altogether 528 OD pairs. After expanding the network, we have $24 \times 2 = 48$ nodes and $76 \times 3 = 228$ arcs. This gives the total number of x_a^k variables equal to $228 \times 528 = 120,384$, plus the number of constraints and their multipliers. This turns out to be too large a problem to be solved using KNITRO. Therefore we reduced the problem size by considering only a subset of the OD pairs.

When reading the trip file (with 528 OD pairs), an acceptance rate of 30% was applied that randomly generated 149 OD pairs. Further, we used the same parameter settings as shown in Table 1, except for "free flow time" and "arc capacity (threshold)" (given by the network file of Sioux-Falls), and "demand" (given by the trip file of Sioux-Falls). Note that the total demand in the network is approximately only 30% out of the original input (149 out of the 528 OD pairs). Hence the arc capacity c_a is divided by 10 based on the original input in order to make the arcs more congested, pushing people to participate in ridesharing.

The values of y_a, η_a^+ and η_a^- can be found in the Appendix, where we see that the ridesharing capacity constraint is satisfied for each original arc $a_0 \in \mathcal{A}_0$, i.e. $y_{a_2} \leq y_{a_3} \leq C y_{a_2}$, for all $a_0 \in \mathcal{A}_0$, $a_2 = \mathcal{T}_2(a_0)$, and $a_3 = \mathcal{T}_3(a_0)$. For most arcs, these constraints hold strictly with the corresponding $\eta_a^+ = \eta_a^- = 0$. Only for arc $a = 46 \in \mathcal{A}_0$, we have $\eta_a^+ = 0.3773 > 0$ and $y_{a_2} = y_{a_3}$, meaning the arc is saturated for ridesharing drivers or passengers. On this arc, we can see the costs of solo drivers, ridesharing drivers and passengers, which are 4.3426, 3.9653 and 4.7200, respectively. In other words, the cost of ridesharing drivers are the lowest among the three. That is why the flow is saturated above for ridesharing drivers on this arc. For all other arcs, the costs of both drivers are always the same, and it is either larger or smaller than the cost for passengers.

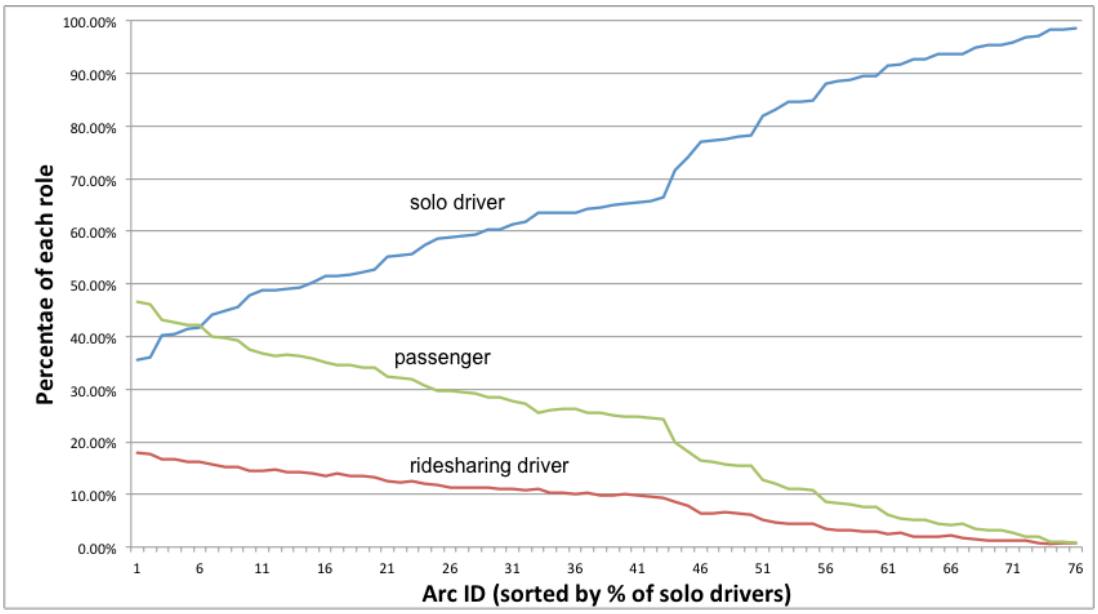

Figure 4: Proportions of solo drivers, ridesharing drivers and passengers for Sioux-Falls

In particular, Figure 4 shows the proportion of each role (solo driver, ridesharing driver or passenger) for each arc in the original graph. According to our model, it is impossible to calculate such proportions for each OD pair because people may change roles throughout their travel. That is, one traveler may be switching from a solo driver to a ridesharing driver along the (actual) path. Or in our model description, one path may contain arcs from different arc sets $\mathcal{A}_1$ and $\mathcal{A}_2$. Figure 4 helps us to understand the distribution of the different roles at a point where travelers will not change roles in a single arc. From this figure, we can see that for some arcs, there are very few people participating in the ridesharing activities, while for some other arcs, the sum of the number of ridesharing drivers and passengers makes up more than half of the total number of travelers passing those arcs. In general, the arcs with higher proportions of solo drivers usually have lower proportions of ridesharing drivers and passengers. For example, compare arc #1 and arc #21, which could indicate that arc #21 is relatively less crowded than arc #1 so less people are participating in ridesharing. However, there are also exceptions – see arc #33 and arc #35. Arc #35 has higher proportion of solo drivers and lower proportion of passengers, *yet* it has *higher* proportion of ridesharing drivers than arc #33. So an increase in solo drivers (proportion) does not necessarily result in a decrease in both ridesharing drivers and passengers.

Also if we take the average of the amount of flow on each type of arc, we can see (from Figure 5)

that on average, the proportions of solo drivers, ridesharing drivers and passengers are 70%, 9%, and 21%. In other words, on average 21% of the travelers will become passengers, reducing the traffic congestion by 21% in the amount of travelers.

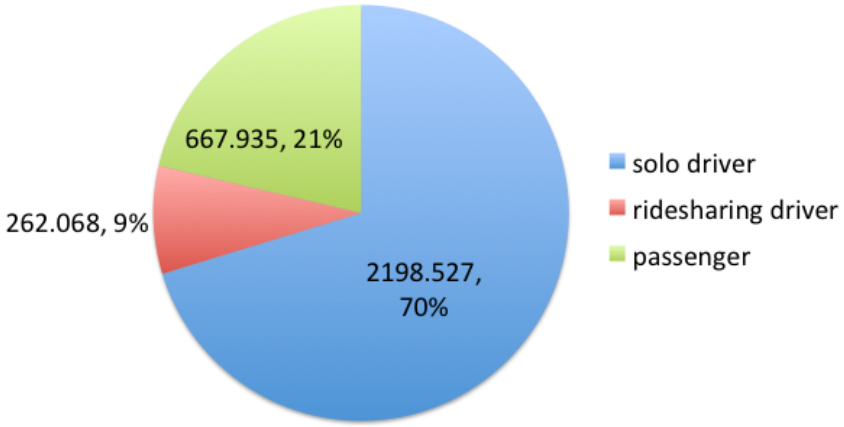

Figure 5: Average proportions of solo, ridesharing drivers and passengers for Sioux-Falls

5.3.1 Path selection analysis

In the test cases of the three-node network and the Braess network, it is not clear if ridesharing drivers have been taking on passengers from other OD pairs. It is because either the network is too simple (Three-node) or there is only one OD pair (Braess). Therefore with the network of Sioux-Falls, we may analyze such activities among the different OD pairs.

Consider only arcs $1, 2 \in \mathcal{A}_0$ in the original graph (see Figure 6), i.e. arc "$1 \to 2$" labeled by "1" and arc "$1 \to 3$" labeled by "2".
Table 7 gives the detailed flow distribution x_a^k over all OD pairs on these two arcs. In this table, the rows are for OD pairs $k \in \mathcal{K}$ and the columns are for arcs $a \in \mathcal{A}$ (after extension). OD pairs with zero flow on these arcs are omitted.

From Table 7 we can see that all the passengers on arc "$1 \to 2$" come from OD pair $k = 12$, i.e. starting from node 3 and traveling to node 8. The number of passengers (96.12) on this arc is far above the capacity that the ridesharing drivers (4.47) from the same OD pair ($k = 12$) can take on. On the other hand, there are several other OD pairs, such as $k = 2, 7, 66, 67$, etc., that do not have passengers, but have ridesharing drivers traveling from node 1 to node 2. These drivers will take on the rest of the passengers that those 4.47 drivers from OD pair $k = 12$ could not. Similarly, on arc "$1 \to 3$", OD pairs $k = 3, 5, 36$ contribute a total of 96.06 passengers, which will be spread out to drivers from the other OD pairs.

It is interesting to note that some seemingly unrelated OD pairs are also using arcs "$1 \to 2$" and "$1 \to 3$". For instance, when $k = 88$, traveling from node 17 to node 2, some travelers will make their path through arc "$1 \to 2$". Note that from the input file the demand, or the total number of travelers, of this OD pair is 200, which is much greater than the number of travelers on arc "$1 \to 2$", i.e. $66.71 + 5.31 = 72.02$. This indicates that drivers will make a detour like this due to traffic congestion, or to pick up passengers from other OD pairs for their own benefit.

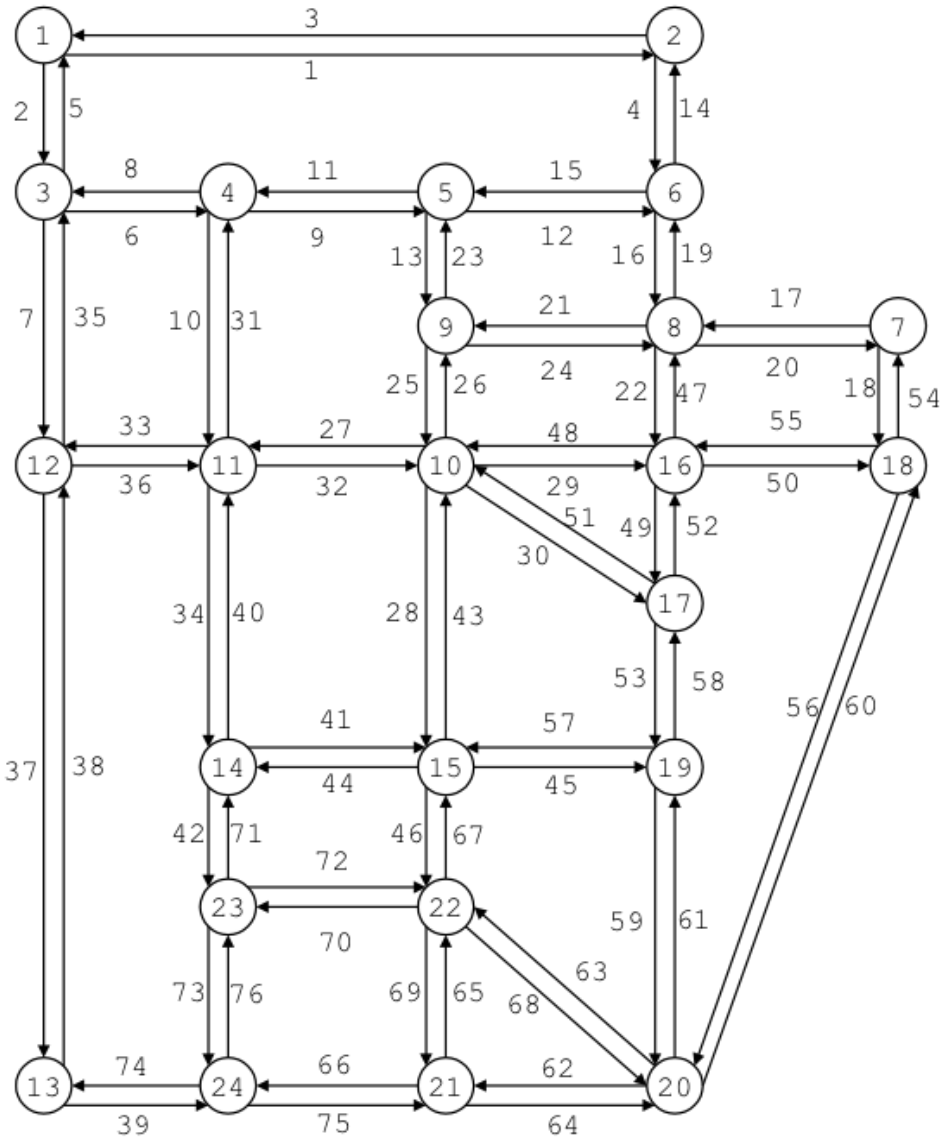

Figure 6: The original network of Sioux-Falls

5.3.2 Sensitivity analysis

As mentioned earlier in Subsection 5.3, for the instance of the Sioux-Falls network solved, we did not adopt the original full input but took only a subset of the OD pairs; we also reduced the arc capacities by ten times. These settings can have an impact on the solution, or the distribution of the flows, i.e. how people will choose their paths. Hence we are interested in checking how the solution will change according to different parameter settings.

Changing the arc capacities c_a. The capacity of each arc c_a is essential to the solution of the model, since it helps to determine the congestion cost for every traveler, which will interfere with

Table 7: Selected x_a^k on the first two original arcs for Sioux-Falls

k	o_k	d_k	arc "1" $\in \mathcal{A}_0$, $1 \to 2$			arc "2" $\in \mathcal{A}_0$, $1 \to 3$		
			$(1,2)_1$	$(1,2)_2$	$(1,2)_3$	$(1,3)_1$	$(1,3)_2$	$(1,3)_3$
1	1	5	0.00	0.00	0.00	196.24	3.76	0.00
2	1	6	294.34	5.66	0.00	0.00	0.00	0.00
3	1	11	0.00	0.00	0.00	490.16	3.81	6.03
4	1	13	0.00	0.00	0.00	496.19	3.81	0.00
5	1	14	0.00	0.00	0.00	273.05	3.78	23.16
6	1	19	0.00	0.00	0.00	296.21	3.79	0.00
7	1	20	171.69	5.58	0.00	119.01	3.72	0.00
9	2	9	0.00	0.00	0.00	196.24	3.76	0.00
10	2	11	0.00	0.00	0.00	196.24	3.76	0.00
12	3	8	19.90	4.47	96.12	0.00	0.00	0.00
27	6	13	0.00	0.00	0.00	196.24	3.76	0.00
33	6	21	0.00	0.00	0.00	96.31	3.69	0.00
34	6	22	0.00	0.00	0.00	33.74	3.45	0.00
36	7	3	0.00	0.00	0.00	29.74	3.40	66.86
66	12	16	657.07	5.72	0.00	0.00	0.00	0.00
67	12	18	160.58	5.57	0.00	0.00	0.00	0.00
78	15	2	94.56	5.44	0.00	0.00	0.00	0.00
88	17	2	66.71	5.31	0.00	0.00	0.00	0.00
132	22	2	94.56	5.44	0.00	0.00	0.00	0.00
146	24	6	69.64	5.33	0.00	0.00	0.00	0.00
y_a			1629.04	48.53	96.12	2619.35	44.50	96.06

people's decision on which type of role to travel. In the BPR functions (1) and (2), i.e.

$$\begin{aligned} tt_a(\boldsymbol{y}) &= t_a \left(1 + b \left(\frac{y_{a_1} + y_{a_2}}{c_a} \right)^4 \right), && a \in \mathcal{A}_1 \cup \mathcal{A}_2 \\ tt_a^{\mathrm{p}}(\boldsymbol{y}) &= t_a \left(1 + b' \left(\frac{y_{a_1} + y_{a_2} + e y_{a_3}}{c_a} \right)^4 \right), && a \in \mathcal{A}_3 \end{aligned}$$

the arc capacity c_a acts as a threshold of the amount of flow on that arc. If the amount of flow is equal to or below c_a, the congestion cost on arc a would be close to its free flow time t_a. If bigger, however, the congestion cost would increase dramatically as the amount of flow increases. Therefore, if c_a decreases, i.e. the threshold decreases, the arcs would become more congested under the same amount of flow. This would push more travelers to participate in ridesharing activities, meaning an increase in the number of both ridesharing drivers and passengers and thus a decrease in the number of solo drivers.

Table 8 shows the changes with c_a for the different networks. In the table, $\bar{D}$ denotes the average demand, i.e. $\bar{D} \triangleq \dfrac{1}{|\mathcal{K}|} \sum_{k \in \mathcal{K}} D_k$. This average can help understand how many people are traveling on the road. Thus we set c_a to be proportional to $0.1\bar{D}$, $\bar{D}$ and $10\bar{D}$, respectively. The triplet in each cell gives the proportions (in %) of solo drivers (SD), ridesharing drivers (RD), and passengers (P). As expected, when c_a increases (from $\sim 0.1\bar{D}$ to $\sim 10\bar{D}$), the proportion of solo drivers increases

while that of ridesharing drivers and passengers decreases. Note that other parameters remain unchanged in this subsection. It can be summarized from Table 8 that when the traffic becomes less congested (as c_a increases), fewer people would participate in ridesharing.

Table 8: Ridesharing proportions (%) with arc capacity changes

	$c_a \sim 0.1\bar{D}$			$c_a \sim \bar{D}$			$c_a \sim 10\bar{D}$		
Test case	% SD	% RD	% P	% SD	% RD	% P	% SD	% RD	% P
Three-node	9.60	31.80	58.61	84.12	7.94	7.94	84.37	7.81	7.81
Braess	0.00	20.00	80.00	0.00	20.00	80.00	20.67	29.33	50.00
Sioux-Falls	15.56	22.82	61.62	70.27	8.38	21.35	99.56	0.22	0.22

When c_a increases, i.e. the congestion cost decreases, more people would become solo drivers while less people will become ridesharing passengers. Note that as the arc capacity increases, the proportion of ridesharing drivers may increase or decrease, but overall the adoption of ridesharing, i.e. the sum of the proportion of ridesharing drivers and passengers, still decreases.

Changing the inconvenience parameters β^{d}, γ^{d}, β^{p}, γ^{p}. The convenience costs of ridesharing for both drivers and passengers are defined in Section 3 by (3) and (4), respectively, i.e.

$$I_a^{\mathrm{d}}(\boldsymbol{y}) = \beta^{\mathrm{d}} y_{a_2} + \gamma^{\mathrm{d}} y_{a_3}, \qquad a \in \mathcal{A}_2$$
$$I_a^{\mathrm{p}}(\boldsymbol{y}) = \beta^{\mathrm{p}} y_{a_2} + \gamma^{\mathrm{p}} y_{a_3}, \qquad a \in \mathcal{A}_3.$$

They are both (linearly) increasing functions of the amount of flow (note that all coefficients are positive). Intuitively, when the inconvenience cost increases, the cost of ridesharing goes up for both drivers and passengers. Hence less people would like to participate in ridesharing; and vice versa.

Note that all the parameters of the inconvenience costs β^{d}, γ^{d}, β^{p}, γ^{p} must satisfy the constraints in (27) to ensure the uniqueness of the arc-flow solution. Thus define

$$\text{Con1} \triangleq 4(\beta^{\mathrm{d}} + \alpha v)(\gamma^{\mathrm{p}} + w) - (\gamma^{\mathrm{d}} - \alpha w + \beta^{\mathrm{p}} - v)^2$$
$$\text{Con2} \triangleq 4eb - b'(1 + eC)^3.$$

When changing any parameters involved above, we need to check if the two inequalities (27) are violated. In changing the arc capacities c_a, however, there is no need to check these constraints since c_a is not involved. In the previous tests, (β^{d}, γ^{d}, β^{p}, γ^{p}) is set to be (0.1, 0.01, 0.1, 0.01). To compare with this settings while maintaining the above two constraints, we multiply (β^{d}, γ^{d}, β^{p}, γ^{p}) by 0.1 and 10, respectively.

The three sets of parameter values are listed in Table 9 and the test results are given in Table 10. We can see that all three sets of (β^{d}, γ^{d}, β^{p}, γ^{p}) satisfy the two parameter requirements (due to positive Con1 and Con2 values). The column title (0.01, 0.001) represents the set ($\beta^{\mathrm{d}} = \beta^{\mathrm{p}} = 0.01$, $\gamma^{\mathrm{d}} = \gamma^{\mathrm{p}} = 0.001$).
In the result of Table 10, c_a is set to $\sim 0.1\bar{D}$ in the "Three-node" network, $\sim 10\bar{D}$ in the "Braess" network, and $\bar{D}$ in the "Sioux-falls" network. This is because the original setting $c_a \sim \bar{D}$ for the first two networks will give ridesharing flows that touch their upper/lower bounds (saturated arcs/paths). These are extreme cases for ridesharing activities where the actual travel costs (NOT the generalized cost) of different travelers are not equal at the equilibrium. Hence different c_a values

Table 9: Parameter settings and constraint checks for inconvenience parameter changes

β^d	γ^d	β^p	γ^p	α	C	ρ	v	w	e	Con1	Con2
0.01	0.001	0.01	0.001	2	4	0.5	0.2	0.1	0.3	0.0143	0.1352
0.1	0.01	0.1	0.01	2	4	0.5	0.2	0.1	0.3	0.1359	0.1352
1	0.1	1	0.1	2	4	0.5	0.2	0.1	0.3	0.6300	0.1352

Table 10: Ridesharing proportions (%) with inconvenience parameter changes

(β, γ)	(0.01, 0.001)			(0.1, 0.01)			(1, 0.1)		
Test case	% SD	% RD	% P	% SD	% RD	% P	% SD	% RD	% P
Three-node	0.00	37.11	62.89	9.60	31.80	58.61	42.19	11.56	46.25
Braess	17.15	32.85	50.00	20.67	29.33	50.00	25.00	25.00	50.00
Sioux-Falls	45.72	17.92	36.36	70.27	8.38	21.35	89.17	2.17	8.66

are selected for the "Three-node" network and the "Braess" network to eliminate this influence. We only consider the situation where the vehicle capacity constraints hold strictly, and thus drivers and passengers may switch roles more willingly. Despite different c_a values for the different networks, all the parameter settings remain fixed except for the inconvenience-cost parameters $(\beta^d, \gamma^d, \beta^p, \gamma^p)$.

From Table 10 we can see that as the inconvenience cost increases, i.e. parameter settings changes from (0.01, 0.001) to (1, 0.1), the proportion of ridesharing decreases (including both drivers and passengers), which meets our expectation. When the inconvenience cost increases, more people would become solo drivers while less people will become ridesharing drivers or passengers.

Changing the pricing parameters ρ, v, w. Changing the pricing parameters can be tricky compared to changing the other parameters. When the price increases, it is appealing for more travelers to become ridesharing drivers. At the same time, however, it may lose passengers as well due to a higher cost being a passenger. Therefore the proportion of ridesharing can either be increasing or decreasing with the changes of pricing parameters.

Same as before, we kept the other parameters fixed while changing any pricing parameters. We set $c_a \sim 0.1\bar{D}$ for the "Three-node" network, $c_a \sim 10\bar{D}$ for "Braess" and $c_a \sim \bar{D}$ for "Sioux-Falls". Still, we set $b' = 0.1b$ for all arcs in all networks. The sets of parameter values are listed in Table 11 and we can see that all parameter settings satisfy all the parameter constraints. The obtained results are given in Table 12.

Table 11: Parameter settings and constraint checks for pricing parameter changes

β^d	γ^d	β^p	γ^p	α	C	ρ	v	w	e	Con1	Con2
0.1	0.01	0.1	0.01	2	4	0.05	0.02	0.01	0.3	0.0063	0.1352
0.1	0.01	0.1	0.01	2	4	0.5	0.2	0.1	0.3	0.1359	0.1352
0.1	0.01	0.1	0.01	2	4	5	2	1	0.3	1.4319	0.1352

From Table 12, we can see that, when the pricing parameters increase there is a significant increase in the number or proportion of ridesharing drivers, while that of passengers decreases as expected. The proportion changes of solo drivers to the pricing parameters are not obvious.

- For "Three-node", the proportion of solo drivers keeps decreasing with the increase of pricing parameters. This means that the benefit as a ridesharing driver appears to be so compelling

Table 12: Ridesharing proportions (%) with pricing parameter changes

(ρ, v, w)	(0.05, 0.02, 0.01)			(0.5, 0.2, 0.1)			(5, 2, 1)		
Test case	% SD	% RD	% P	% SD	% RD	% P	% SD	% RD	% P
Three-node	21.41	15.72	62.87	9.60	31.80	58.61	5.37	38.61	56.02
Braess	0.33	20.07	79.61	20.67	29.33	50.00	12.87	37.13	50.00
Sioux-Falls	68.50	6.30	25.20	70.27	8.38	21.35	70.37	9.90	19.73

that both solo drivers and passengers would switch to be a ridesharing driver.

- For "Braess", the proportion of solo drivers increases when the price parameters increase from (0.05, 0.02, 0.01) to (0.5, 0.2, 0.1), because this change has more of an impact on passengers than on drivers, and thus more passengers are switching to solo drivers than to ridesharing drivers. In other words, the decrease of the proportion of passengers overcomes the increase of the proportion of ridesharing drivers. Therefore the overall proportion of ridesharing decreases, which leads to an increase of solo drivers.

- For "Sioux-Falls", the proportion of solo drivers keeps increasing with the increase of the ridesharing price parameters. Similar to the first half of the case for "Braess", an increase in these parameters pushes more passengers to drive alone than to drive with other passengers.

Summary. The changes with the parameter settings can be summarized in Table 13, where the first column represents different traveler roles ("ridesharing (total)" includes both ridesharing drivers and ridesharing passengers), and the second to the fourth columns give the proportion changes for each role under different parameter changes.

Table 13: The impact of parameter changes on ridesharing proportions

Proportion changes	arc capacity ↑	inconvenience cost ↑	pricing parameters ↑
solo driver	↑	↑	undetermined
ridesharing (total)	↓	↓	undetermined
driver	undetermined	↓	↑
passenger	↓	↓	↓

It can be observed from Table 13 that

1. When the arc capacity increases, more people would become solo drivers and thus less people would participate in ridesharing. Passengers will become solo drivers or ridesharing drivers.

2. When the inconvenience cost increases, more people would become solo drivers and thus less people would participate in ridesharing. In particular, both the number of ridesharing drivers and passengers will decrease due to an increased cost.

3. When the ridesharing price parameters increase, more people would become ridesharing drivers and less people would become ridesharing passengers. The number of solo drivers is undetermined, that is, it is possible that more passengers are switching to solo drivers, and it is also likely that more solo drivers would become ridesharing drivers.

These sensitivity results validate that the proposed model correctly captures reasonable behavior, such as increasing arc capacity leads to an increase in solo drivers and decrease in ridesharing

passengers. However, there are some unexpected or undetermined results. For example increasing ridesharing pricing parameters for the Sioux-Falls network example does not have a marked effect on the number of solo drivers and total ridesharing. This implies that if a planner forces an increase in ridesharing price, attempting to make ridesharing drivers more attractive, it could lead to an overall increase in drivers and a reduction in total ridesharing, increasing congestion.

6 Conclusions

This paper proposes VI/CP models for solving the traffic equilibrium problem with ridesharing. The mathematical models developed explicitly take into account how the notion of shortest path has to be adapted to include the costs/benefits of ridesharing and provide a method to quantify these costs. These models determine how travelers will behave given a transportation system with ridesharing services, and hence help city planners to design certain conditions according to travelers' behavior in order to reduce traffic congestion. In our study, we made some assumptions, such as (a) the drivers and passengers that are sharing the same car may travel on different OD pairs; (b) there is a vehicle capacity constraint for all ridesharing vehicles. In order to cope with (a), the travel network is extended by doubling the size of the node set and tripling the size of the arc set; to handle (b), a generalized traffic equilibrium is defined and is formulated as a mixed complementarity problem and also equivalently as a variational inequality. The latter is shown to have a unique solution. The KNITRO solver is adopted to solve the resulting MiCP. The computational results are also promising, as not only do they validate some intuitive guesses, but also provide new insights to some unexpected conclusions.

Future challenges may include: (1) an individual level transportation equilibrium model with ridesharing, such that the assignment of each passenger may be captured; (2) an inconvenience cost based on paths instead of arcs; (3) more transit modes (like public transit) for travelers to choose from; (4) elastic traffic demand where travelers may choose not to travel if no transit modes meet their needs; etc.

Acknowledgment

The work of Xu, Dessouky, and Ordóñez was based on research supported by the Federal Highway Administration under the Broad Agency Announcement of Exploratory Advanced Research (EAR). The work of Pang was based on research supported by the U.S. National Science Foundation under grant CMMI-1402052.

References

[1] Aashtiani, H. and Magnanti, T. Equilibria on a congested transportation network. *SIAM Journal on Algebraic Discrete Methods* 2 (1981) 213–226.

[2] Agdeppa, R.P., Yamashita, N., and Fukushima, M. The traffic equilibrium problem with nonadditive costs and its monotone mixed complementarity problem formulation. *Transportation Research Part B: Methodological* 41 (2007) 862–874.

[3] Amey, A. Real-time ridesharing : exploring the opportunities and challenges of designing a technology-based rideshare trial for the MIT community. Master's thesis. Massachusetts Institute of Technology (2010).

[4] Ban, X., Liu, H., Ferris, M.C., and Ran, B. A link-node complementarity model and solution algorithm for dynamic user equilibria with exact flow propagations. *Transportation Research, Part B: Methodological* 9 (2008) 823–842.

[5] *BTS Transportation Statistics Annual Report 2012*. U.S. Department of Transportation, Research and Innovative Technology Administration Bureau of Transportation Statistics. (2013).

[6] Burris, M. and Winn, J. Slugging in Houston-Casual carpool passenger characteristics. *Journal of Public Transportation* 9 (2006) 23–40.

[7] Byrd, R., Hribar, M.E., and Nocedal, J. An interior point method for large scale nonlinear programming. *SIAM Journal on Optimization* 4 (1999) 877–900.

[8] Byrd, R.H., Nocedal, J., and Waltz, R.A. KNITRO: An Integrated Package for Nonlinear Optimization In G. Di Pillo and R. Noma, editors. *Large-Scale Nonlinear Optimization* 83 (2006) pp. 35–59.

[9] Chan, N. and Shaheen, S. Ridesharing in North America: past, present, and future. *Transport Reviews* 32 (2012) 93–112.

[10] Czyzyk, J., Mesnier, M., and Moré, J. The NEOS server. *IEEE Journal on Computational Science and Engineering* 5 (1998) 68–75.

[11] Dafermos, S.C. Traffic equilibrium and variational inequalities. *Transportation Science* 14 (1980) 42–54.

[12] Dailey, D.J., Loseff, D., and Meyers, D. Seattle smart traveler: dynamic ridematching on the World Wide Web. *Transportation Research Part C: Emerging Technologies* 7 (1999) 17–32.

[13] Dolan, E. The NEOS server 4.0 administrative guide. Mathematics and Computer Science Division, Argonne National Laboratory, Technical Memorandum ANL/MCS-TM-250 (2001).

[14] Facchinei, F. and Pang, J.S. *Finite-Dimensional Variational Inequalities and Complementarity Problems*. Springer (New York 2003).

[15] Ferguson, E. The rise and fall of the American carpool: 1970–1990. *Transportation* 24 (1997) 349–376.

[16] Ferris, M.C. and Munson, T.S. Interfaces to PATH 3.0: Design, Implementation and Usage. *Computational Optimization and Applications* 12 (1999) 207–227.

[17] Furuhata, M., Dessouky, M.M., Ordóñez, F., Brunet, M., Wang, X., and Koenig, S. Ridesharing: the state-of-the-art and future directions. *Transportation Research Part B: Methodological* 57 (2013) 28–46.

[18] Ghoseiri, K., Haghani, A., and Hamedi, M.. Real-time rideshare matching problem. Department of Civil and Environmental Engineering, University of Maryland College Park (January 2011).

[19] Gropp, W. and Moré, J. Optimization environments and the NEOS server. In Buhmann, M.D. and Iserles, A., editors. *Approximation Theory and Optimization*, Cambridge University Press (1997) pp. 167–182.

[20] Heinrich, S. Implementing real-time ridesharing in the San Francisco bay area. Master's thesis, Mineta Transportation Institute, San Jose State University (2010).

[21] Hubbard, R.G. and O'Brien, A.P. *Economics*. Fourth edition. Prentice Hall (2012).

[22] Kelley, K. Casual carpooling—enhanced. *Journal of Public Transportation* 10 (2007) 119–130.

[23] Jayakrishnan, R., Tsai, W.K., Prashker, J.N., and Rajadhyaksha, S. A faster path-based algorithm for traffic assignment. *Transportation Research Record* 1443 (1994) 75–83.

[24] Larsson, T. and Patriksson, M. Side constrained traffic equilibrium models–analysis, computation and applications. *Transportation Research Part B: Methodological* 33 (1999) 233–264.

[25] Larsson, T. and Patriksson, M. Equilibrium characterizations of solutions to side constrained asymmetric traffic assignment models. *Le Matematiche* 49 (1994) 249–280.

[26] LeBlanc, D. Slugging: The Commuting Alternative for Washington DC. *Forel Publishing* (1999).

[27] Levofsky, A. and Greenberg, A. Organized dynamic ride sharing: The potential environmental benefits and the opportunity for advancing the concept. *Transportation Research Board Annual Meeting* (2001).

[28] Lu, S.. Sensitivity of static traffic user equilibria with perturbations in arc cost function and travel demand. *Transportation Science* 42 (2008) 105–123.

[29] Morency, C. The ambivalence of ridesharing. *Transportation* 34 (2007) 239–253.

[30] Nie, Y. A note on Bar-Gera's algorithm for the origin-based traffic assignment problem. *Transportation Science* 46 (2012) 27–38.

[31] Patriksson, M. *The Traffic Assignment Problem: Models and Methods*. CRC Press (1994).

[32] Qian, Z. and Zhang, H.. Modeling multi-modal morning commute in a one-to-one corridor network. *Transportation Research Part C: Emerging Technologies* 19 (2011) 254–269.

[33] Schrank, D., Eisele, W., and Lomax, T. *2012 Urban Mobility Report*. Texas A&M Transportation Institute. `http://d2dtl5nnlpfr0r.cloudfront.net/tti.tamu.edu/documents/mobility-report-2012.pdf`.

[34] Spielberg, F. and Shapiro, P. Mating habits of slugs: Dynamic carpool formation in the I-95/I-395 corridor of Northern Virginia. *Transportation Research Board* 1711 (2000) 31–38.

[35] Wardrop, J. Some theoretical aspects of road traffic research. *Proceeding of the Institute of Civil Engineers, Part II* 1 (1952) 325–362.

[36] Xu, H. *Traffic Assignment Models for a Ridesharing Transportation Market*. Ph.D. Thesis. Department of Industrial and Systems Engineering, University of Southern California (June 2014).

[37] Xu, H., Ordóñez, F., and Dessouky, M. A traffic assignment model for a ridesharing transportation market. *Journal of Advanced Transportation* (December 2014) doi: 10.1002/atr.1300.

[38] Yang, H. and Huang, H.. Carpooling and congestion pricing in a multilane highway with high-occupancy-vehicle lanes. *Transportation Research Part A: Policy and Practice* 33 (1999) 139–155.

APPENDIX: KNITRO Outputs – Sioux Falls, 149 OD pairs

a	y_{a_1}	y_{a_2}	y_{a_3}	η_a^+	η_a^-	f_{a_1}	f_{a_2}	f_{a_3}
1	1,629.04	48.53	96.12	0.0000	0.0000	6.1584	6.1584	14.7375
2	2,619.35	44.50	96.06	0.0000	0.0000	5.0071	5.0071	12.2216
3	1,532.91	37.41	66.86	0.0000	0.0000	6.1216	6.1216	12.6270
4	1,207.02	198.53	496.12	0.0000	0.0000	53.4338	53.4338	49.4649
5	2,055.77	44.53	96.12	0.0000	0.0000	4.3892	4.3892	12.1616
6	4,403.41	172.21	432.12	0.0000	0.0000	34.6830	34.6830	39.7440
7	4,694.50	67.60	156.85	0.0000	0.0000	14.2855	14.2855	17.5631
8	4,702.76	169.48	424.94	0.0000	0.0000	43.4471	43.4471	40.1694
9	3,882.73	74.19	184.70	0.0000	0.0000	9.3544	9.3544	16.6759
10	1,185.85	183.23	450.61	0.0000	0.0000	60.4557	60.4557	48.1802
11	3,726.67	53.20	129.47	0.0000	0.0000	8.1239	8.1239	12.5596
12	1,037.39	86.03	205.35	0.0000	0.0000	19.9440	19.9440	21.9591
13	3,068.18	460.13	1,184.55	0.0000	0.0000	121.2320	121.2320	108.8490
14	1,208.29	243.20	613.68	0.0000	0.0000	60.0843	60.0843	59.5661
15	1,174.97	205.44	519.59	0.0000	0.0000	40.3467	40.3467	48.1865
16	1,748.55	676.07	1,768.62	0.0000	0.0000	182.0600	182.0600	169.6770
17	2,328.10	181.63	462.19	0.0000	0.0000	50.2125	50.2125	43.0318
18	3,376.82	123.78	315.21	0.0000	0.0000	3.5017	3.5017	25.4624
19	1,678.71	374.44	974.84	0.0000	0.0000	94.5799	94.5799	88.5590
20	2,398.82	201.78	515.21	0.0000	0.0000	57.4307	57.4307	47.8525
21	951.38	165.56	383.06	0.0000	0.0000	45.8905	45.8905	45.8905
22	1,197.77	354.05	905.39	0.0000	0.0000	72.0958	72.0958	84.4784
23	2,991.64	480.24	1,237.46	0.0000	0.0000	113.9730	113.9730	111.9570
24	1,016.22	307.36	756.20	0.0000	0.0000	80.7716	80.7716	80.7716
25	4,046.12	208.74	533.52	0.0000	0.0000	42.3296	42.3296	46.8725
26	3,123.36	70.79	170.49	0.0000	0.0000	15.4911	15.4911	17.5062
27	2,970.51	477.57	1,230.45	0.0000	0.0000	111.0170	111.0170	111.0170
28	4,293.75	822.40	2,132.62	0.0000	0.0000	190.9850	190.9850	190.9850
29	1,322.91	652.21	1,695.29	0.0000	0.0000	168.3590	168.3590	168.3590
30	1,067.71	288.76	717.78	0.0000	0.0000	73.3421	73.3421	73.8603
31	959.45	113.87	268.09	0.0000	0.0000	26.5710	26.5710	29.8486
32	3,051.02	580.80	1,502.12	0.0000	0.0000	135.4850	135.4850	135.4850
33	1,161.31	337.90	857.63	0.0000	0.0000	84.3035	84.3035	84.3035
34	1,329.49	669.18	1,739.96	0.0000	0.0000	173.3090	173.3090	173.3090
35	3,899.37	24.15	42.49	0.0000	0.0000	8.7395	8.7395	8.7395
36	1,178.32	304.09	768.66	0.0000	0.0000	80.8532	80.8532	76.4905
37	4,152.62	139.08	350.21	0.0000	0.0000	6.3925	6.3925	29.4888
38	3,581.49	32.36	69.36	0.0000	0.0000	4.7056	4.7056	9.0684
39	1,523.65	521.08	1,350.21	0.0000	0.0000	160.0960	160.0960	134.5790
40	1,315.36	365.46	940.69	0.0000	0.0000	88.6847	88.6847	88.6847

41	1,325.64	549.02	1,418.48	0.0000	0.0000	139.0040	139.0040	139.0040
42	1,084.33	91.88	220.73	0.0000	0.0000	23.5227	23.5227	23.5227
43	3,636.57	302.57	764.67	0.0000	0.0000	71.0087	71.0087	71.0087
44	1,309.14	380.07	973.87	0.0000	0.0000	93.3406	93.3406	93.3406
45	1,853.05	12.52	17.15	0.0000	0.0000	4.2113	4.2113	5.2573
46	1,253.13	8.46	8.46	0.3773	0.0000	4.3426	3.9653	4.7200
47	1,138.61	204.81	512.65	0.0000	0.0000	42.6854	42.6854	49.2246
48	1,470.19	220.22	558.46	0.0000	0.0000	92.1841	92.1841	58.2786
49	716.10	38.37	90.46	0.0000	0.0000	3.2993	3.2993	9.2625
50	4,268.66	53.52	125.06	0.0000	0.0000	13.4697	13.4697	13.9879
51	1,089.16	389.51	982.92	0.0000	0.0000	100.2660	100.2660	100.2660
52	1,789.72	404.87	1,054.93	0.0000	0.0000	95.0164	95.0164	94.4982
53	1,695.39	444.10	1,158.15	0.0000	0.0000	118.0780	118.0780	107.1790
54	3,498.37	78.22	195.33	0.0000	0.0000	3.6364	3.6364	16.8380
55	3,843.30	218.22	558.46	0.0000	0.0000	11.1635	11.1635	45.0689
56	6,326.35	169.27	424.40	0.0000	0.0000	39.6051	39.6051	39.6051
57	4,006.15	205.61	525.29	0.0000	0.0000	34.4664	34.4664	45.3654
58	861.91	10.52	17.15	0.0000	0.0000	5.2094	5.2094	4.1634
59	1,107.55	176.13	442.45	0.0000	0.0000	30.0137	30.0137	40.9127
60	6,754.61	224.51	569.75	0.0000	0.0000	51.4493	51.4493	51.4493
61	1,385.32	360.21	926.88	0.0000	0.0000	92.9352	92.9352	87.9994
62	942.14	99.91	231.34	0.0000	0.0000	22.1889	22.1889	26.5515
63	1,229.47	230.56	580.42	0.0000	0.0000	56.3484	56.3484	56.3484
64	1,224.65	503.24	1,292.73	0.0000	0.0000	128.3870	128.3870	128.3870
65	1,684.28	256.88	665.48	0.0000	0.0000	58.9370	58.9370	58.9370
66	1,494.27	585.01	1,523.72	0.0000	0.0000	150.6660	150.6660	146.3040
67	3,436.99	666.24	1,737.48	0.0000	0.0000	153.2380	153.2380	153.2380
68	1,260.67	284.72	722.94	0.0000	0.0000	69.4498	69.4498	69.4498
69	1,221.47	76.84	191.68	0.0000	0.0000	13.3935	13.3935	17.7562
70	1,375.53	458.09	1,184.45	0.0000	0.0000	112.5210	112.5210	112.5210
71	1,321.24	333.10	855.53	0.0000	0.0000	80.4017	80.4017	80.4017
72	1,319.43	275.79	704.72	0.0000	0.0000	66.1673	66.1673	66.1673
73	1,595.90	224.61	580.55	0.0000	0.0000	51.5392	51.5392	51.5392
74	1,402.69	428.08	1,105.46	0.0000	0.0000	104.3190	104.3190	104.3190
75	1,125.57	208.48	532.83	0.0000	0.0000	28.0216	28.0216	46.1986
76	1,247.19	181.52	467.17	0.0000	0.0000	20.7913	20.7913	38.9683